DOI: 10.1002/cmdc.201000383

Structure–Activity Relationship Refinement and Further Assessment of Indole-3-glyoxylamides as a Lead Series against Prion Disease

Mark J. Thompson, Jennifer C. Louth, Steven Ferrara, Fiona J. Sorrell, Benjamin J. Irving, Edward J. Cochrane, Anthony J. H. M. Meijer, and Beining Chen*[a]

Structure–activity relationships within the indole-3-glyoxylamide series of antiprion agents have been explored further, resulting in discovery of several new compounds demonstrating excellent activity in a cell line model of prion disease (EC_{50} <10 nM). After examining a range of substituents at the *para*-position of the *N*-phenylglyoxylamide moiety, five-membered heterocycles containing at least two heteroatoms were found to be optimal for the antiprion effect. A number of modifications were made to probe the importance of the glyoxylamide substructure, although none were well tolerated. The most potent compounds did, however, prove largely stable towards microsomal metabolism, and the most active library member cured scrapie-infected cells indefinitely on administration of a single treatment. The present results thereby confirm the indole-3-glyoxylamides as a promising lead series for continuing in vitro and in vivo evaluation against prion disease.

Introduction

Prion diseases, or transmissible spongiform encephalopathies (TSEs), are a family of rapidly progressive, invariably fatal, neurodegenerative disorders affecting both humans and animals, for which no effective therapy is currently available. This class of disease is represented by Creutzfeldt–Jakob Disease (CJD), Gerstmann–Sträussler–Scheinker syndrome (GSS), familial fatal insomnia (FFI) and kuru in humans; scrapie in sheep and goats; and bovine spongiform encephalopathy (BSE) in cattle, in addition to several other seldom encountered or emerging TSEs that have been characterised.[1]

Although the precise molecular mechanisms underlying these conditions remain enigmatic, all prion diseases are associated with conversion of normal cellular prion protein (PrP^C), which is expressed predominantly within the central nervous system (CNS), into a pathogenic isoform, denoted PrP^{Sc}. While a full understanding of this refolding event remains elusive despite extensive investigation,[2] the disease-associated PrP^{Sc} conformation of the protein is β-sheet rich and readily oligomerises, leading to precipitation of the fibrillar structures that are a hallmark of clinical TSE cases. It is these deposits of PrP^{Sc} that are thought to be, either directly or indirectly, a cause of neuronal cell death and disease progression.

A number of cell lines persistently infected with TSE agents have been routinely used as a disease model in screening campaigns for small-molecule antiprion agents,[3] and as such, inhibition of PrP^{Sc} propagation in these in vitro systems is the first step in identifying potential prion disease therapeutics. The scrapie mouse brain (SMB) cell line,[4,5] established by culture from the brain of a mouse infected with the Chandler scrapie strain and shown to be of mesodermal origin, provides one such model suitable for initial screening work.

We recently described a series of indole-3-glyoxylamides as highly effective antiprion agents in the SMB cell line.[6] The most active compounds displayed low nanomolar EC_{50} values (Figure 1a), and a general requirement was recognised for a *p*-substituted aniline moiety at the glyoxylamide position, ideally containing at least one hydrogen-bond acceptor. Substitution at the indole C-2 was not tolerated. In addition, a small number of 1-methylindole analogues of active compounds revealed a lessening of activity by approximately an order of magnitude, though the 1-methyl derivatives of the most active library members were not included in the original study. To build upon this earlier work, a number of second generation libraries have been designed and evaluated to further our understanding of structure–activity relationships in the indole-based series of antiprion compounds (Figure 2).

Firstly, additional *p*-substituted aniline-derived compounds (**1g–p**) related to **1a–f** were prepared to enrich our understanding of the requirements for optimal activity at this position, focusing on variation of the 5-membered heterocyclic substituent present in several of the most active compounds (**1a–b**, **1e**). It was also planned to synthesise analogues of **1** with either carbonyl oxygen sequentially removed (**2** or **3**), to ascertain the relative contribution of each towards the observed biological activity. In addition, we wished to investigate whether any scope existed for further modification of the

[a] *Dr. M. J. Thompson, J. C. Louth, S. Ferrara,[+] F. J. Sorrell, B. J. Irving, E. J. Cochrane, Dr. A. J. H. M. Meijer, Dr. B. Chen*
Department of Chemistry, University of Sheffield
Brook Hill, Sheffield, S7 3HF (UK)
Fax: (+44) 114-2229346
E-mail: b.chen@sheffield.ac.uk

[+] *present address: University of Oxford, Chemistry Research Laboratory 12 Mansfield Road, Oxford, OX1 3TA (UK)*

Supporting information for this article is available on the WWW under http://dx.doi.org/10.1002/cmdc.201000383.

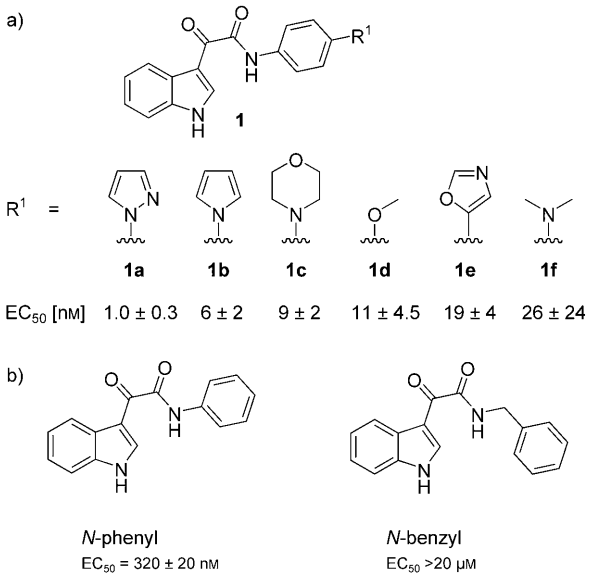

Figure 1. a) Indole-3-glyoxylamides **1a**–**f** identified as potent antiprion agents; b) Additional parent compounds selected for synthesis of further analogues.

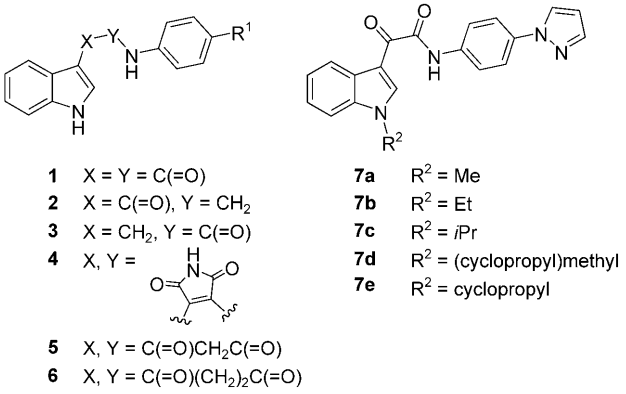

Figure 2. Compound series devised to further probe antiprion structure–activity relationships at positions 1 and 3 of the indole ring.

glyoxylamide motif, by preparing series of analogues either replacing the dicarbonyl moiety by a heterocycle (**4**), or inserting a bridging group between the two carbonyl functions (**5** and **6**).

For series **2**–**6**, a small subset of R^1 substituents was chosen prioritising ease of synthesis in the first instance, with the initial goal of ascertaining whether any of the modified analogues were worthy of further development. Hence, structures **1c** and **1d** were selected as parent compounds for these new libraries, together with the *N*-phenyl derivative ($R^1 = H$, $EC_{50} = 0.32$ μM;[6] Figure 1b), to represent a range of activities. Analogues of one inactive parent molecule, *N*-benzyl-2-(1*H*-indol-3-yl)-2-oxoacetamide, were also proposed, to ascertain whether any of the new modifications might be able to improve the performance of this compound. Direct analogues of heteroaryl-substituted derivatives such as **1a** and **1e** were not prioritised at this stage, since these compounds presented problems with solubility during synthesis, such that direct analogues would only be added to the most promising compound series.

Finally, a series of 1-alkyl analogues (**7a**–**e**) of present lead compound **1a** was prepared, to elucidate the largest group that could be accommodated at the indole N-1 position whilst still maintaining an acceptable degree of biological activity, since only 1-methyl derivatives had been evaluated up to this point.

Results and Discussion

Variation at the *para*-position of the aniline ring

Indole-3-glyoxylamides **1g**–**p** (Table 1) were prepared using essentially the same methodology as employed for the earlier compounds **1a**–**e**, and related libraries.[6] Consecutive reaction of indole with oxalyl chloride followed by the appropriate *p*-substituted aniline provided the desired products in a two-step, one-pot procedure. During the latter step, 2,6-lutidine was employed as a base in the given examples as it had been found to give improved yields as compared to Hünig's base (*N*,*N*-diisopropylethylamine, DIPEA) in some cases. The low yields obtained for several examples (<10%) were seemingly a

Table 1. Antiprion screening results for compounds **1g**–**p**.

Compd	R^1	Yield [%]	EC_{50}[a] [nM]
1g		6	4.3 ± 0.8
1h		3	1.3 ± 0.2
1i	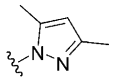	45	109 ± 65
1j		3	4.4 ± 2.8
1k		16	125 ± 21
1L	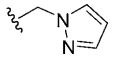	42	667 ± 444
1m		4	1.1 ± 0.2
1n	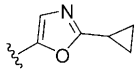	14	36 ± 25
1o		23	21 ± 4
1p		9	–[a]

[a] Values represent the mean ± SD of at least two experiments, each performed in triplicate. [b] Toxic to cells at all test concentrations: 1, 10, 20 μM.

consequence of poor solubility of the parent anilines or the final compounds during the reaction and work-up sequence.

Screening results indicated that all of the new indole-3-glyoxylamides were active antiprion agents, with varying degrees of potency, with the exception of **1p**, whose activity could not be assessed due to toxicity of the compound towards the cells. Comparison of pyrrolidino derivative **1k** (EC_{50} = 125 nM) with its pyrrol-1-yl analogue **1b** (EC_{50} = 6 nM) indicates a strong preference for an unsaturated, aromatic system; indeed, several compounds bearing a heteroaryl group at the R^1 position are more potent than the best unsaturated compound (**1c**, R^1 = morpholino, EC_{50} = 9 nM). Inserting a methylene bridge between the aniline ring and the *p*-pyrazol-1-yl substituent of **1a** (EC_{50} = 1 nM), as in analogue **1l**, is also greatly detrimental to activity. Thus, a fairly stringent requirement for a direct-linked heteroaromatic system at the R^1 position of **1** is evident for optimal cell-line activity.

Exploring further the nature of the heterocycle, some conclusions can be drawn. Imidazol-1-yl derivative **1h** is just as potent as the pyrazol-1-yl parent **1a**; however, 1,2,4-triazol-1-yl compound **1g** proved marginally less effective. Introducing 3,5-dimethyl substitution to the pyrazole ring of **1a** resulted in a drop of activity by two orders of magnitude (**1i**, EC_{50} = 109 nM). Modifications to oxazol-5-yl compound **1e** were also explored. Removing the nitrogen atom was of little consequence, since 2-furyl analogue **1o** was equally as active as its oxazole parent, whereas introducing a cyclopropyl substituent at C-2 compromised effectiveness to some extent (**1n**, EC_{50} = 36 nM). Potency was considerably improved by incorporating an additional ring nitrogen, with 1,3,4-oxadiazol-1-yl compound **1m** equalling the activity of the present lead **1a**.

In summary, the substituent R^1 of indole-3-glyoxylamides **1** should optimally be a 5-membered aromatic ring containing at least two heteroatoms. Evidence thus far indicates that if additional heteroatoms are present, then at least one should be oxygen. Further substitution of the heterocycle is generally a disadvantage, since only 1-methylpyrazol-3-yl derivate **1j** displayed activity comparable with that of the most potent compounds, which all contain unsubstituted systems.

Computational analysis of factors influencing activity

In order to gain further insight into the above results, the electronic properties of several members of lead series **1** were investigated by in silico methods. Calculations were performed using the SMP version of the Gaussian 09 package, employing the B3LYP functional method, and the 6-311G(d,p) basis set on all atoms. Optimisations were carried out in vacuo, and electrostatic potential (ESP) surfaces were plotted using GaussView between the limits of −5.0 and +5.0 atomic units. ESPs were generated for structures **1a**–**k**, **1m** and **1o**, together with a handful of additional examples from our previous report:[6] **1q**–**v** (where R^1 = piperidin-1-yl, SMe, OCF_3, Me, OH and F, respectively). Since hydrogen-bond acceptor character of the *p*-substituent (R^1 position) had previously been postulated as important in contributing to activity,[6] the calculated ESPs were inspected for any obvious correlation between electronic properties and antiprion EC_{50} values.

Within the most interesting subset of compounds—those bearing an unsubstituted 5-membered ring at the key R^1 position—a qualitative relationship was seen between increasing EC_{50} values and growing negative character of the glyoxylamide-linked aromatic ring (Figure 3). No firm conclusions could be drawn across the set of test compounds as a whole, however, steric factors evidently also play an important role. Analogue **1f** (R^1 = NMe_2) is five times more potent than the closely related structure **1k** (R^1 = pyrrolidin-1-yl), even though the electronic characteristics of the benzene ring are essentially identical in these two examples.

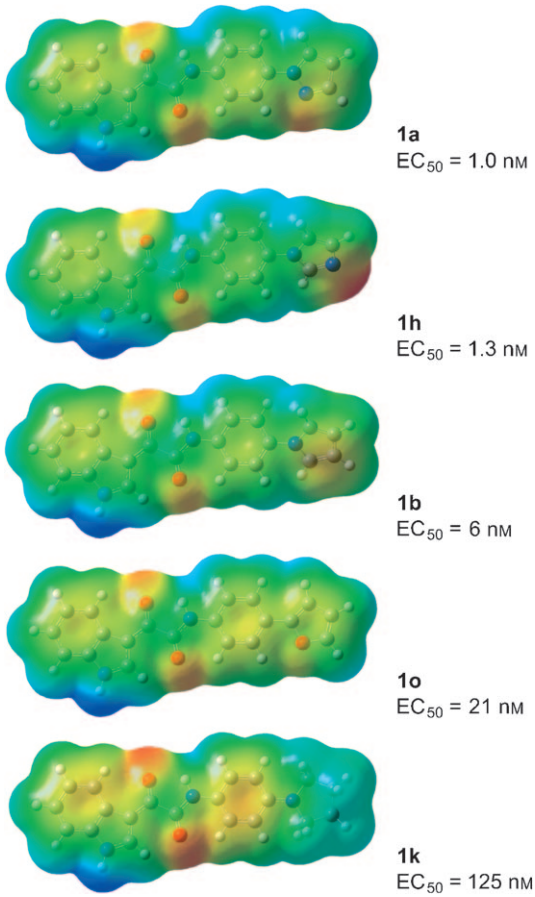

Figure 3. Electrostatic potential (ESP) surfaces of five compounds containing an unsubstituted 5-membered ring at the crucial R^1 position; these derivatives have varying antiprion potency. As the observed EC_{50} value increases, a concurrent increase in negative charge (i.e., electron density) of the attached aromatic system can be seen, represented in the ESP surface as a gradual colour change from green→yellow→orange over the benzene ring.

Therefore, further analysis was deemed necessary in order to better understand factors contributing to the biological activity of the indole compounds, with particular attention paid to the aforementioned supposition over hydrogen-bond acceptor ability. Inspired by a recent study investigating similar characteristics of a series of triazole-based dopamine D_3 receptor antagonists,[7] point charges (in the form of atom partial charges)

were computed for both the *p*-substituent atom and *p*-carbon atom of each ESP surface.

Examining the series of partial charges at each position alone showed no discernible trend. However, considering the polarisation of the C–R^1 bond, defined in this case as the difference in partial charges between the substituent atom and *p*-C atom, a clear correlation became obvious (Figure 4a). Activity is more strongly favoured where this difference is positive (i.e. the substituent atom is more $\delta+$), and all the compounds where this is the case demonstrate EC_{50} values of 21 nM or less. In contrast, related structures where the C–R^1 bond is polarised in the opposite sense show EC_{50} values distributed over a much wider range, suggesting this electronic characteristic is generally detrimental to the desired antiprion effect of the indole-3-glyoxylamides. Although not entirely conclusive, the above results do suggest future analogues should be designed with this bond polarised in a specific sense for optimal effect, which in turn will allow the supposition to be tested further.

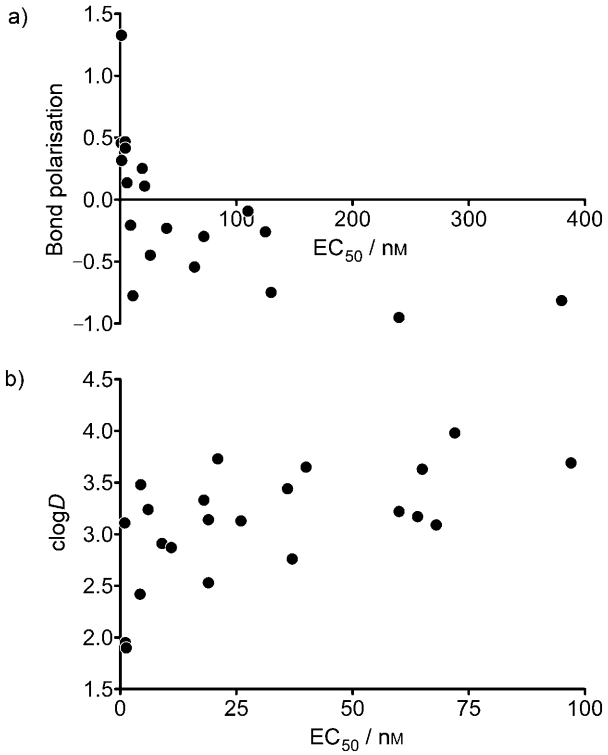

Figure 4. Scatter plots illustrating the observed correlation between: a) antiprion EC_{50} value and C–R^1 bond polarisation (Pearson *r* value = −0.618; *P* value = 0.005); and, b) EC_{50} value and clog *D* (Pearson *r* value = 0.566; *P* value = 0.006). Computed R^2 values for the plots are a) 0.3818 and b) 0.3208. Bond polarisation is defined as the difference in partial ESP charges between the two atoms of the C–R^1 bond.

In an associated analysis, the interdependence between activity and lipophilicity was explored, considering the most promising leads of type **1** reported to date (where EC_{50} < 100 nM). A clear correlation between EC_{50} and clog *D*[8] values was evident for these structures (Figure 4b), with the more hydrophobic compounds tending to be less potent. Thus, a number of factors favouring activity of the lead series have been identified, which are expected to aid the design of improved analogues during concomitant optimisation of both antiprion efficacy and pharmacokinetic properties. Ideally, R^1 should be a 5-membered heterocycle that does not donate electron density into the adjacent aromatic ring; the C–R^1 bond should be polarised in a particular sense; and the optimal clog *D* value for this series appears to lie in the range 2.0–3.0. With the above conclusions in place, variations to the glyoxylamide substructure of **1** were then explored, to ascertain the importance of this motif in contributing to the observed biological activity.

Modifications to the glyoxylamide substructure

Systematic replacement of either glyoxylamide carbonyl by a methylene group was investigated as discussed above, in order to gain understanding of their relative contribution towards antiprion activity. Analogues **2a–d**, retaining the carbonyl moiety adjacent to the indole 3-position, were prepared by reaction of indole with chloroacetyl chloride,[9] followed by displacement of chloride by each of a small set of amines (Scheme 1a). Related compounds **3a–d**, retaining the alternative carbonyl group, were prepared by straightforward amide coupling reactions between indole-3-acetic acid and the same set of amines (Scheme 1b).

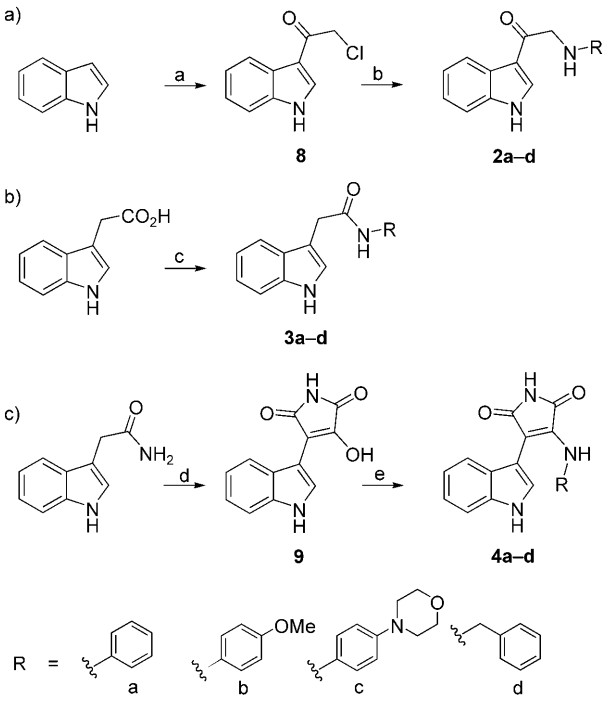

Scheme 1. *Reagents and conditions:* a) $ClCH_2COCl$, pyridine, dioxane, 60 °C, 1 h (13%); b) *i*Pr_2NEt, RNH_2, KI, MeCN, reflux, 18 h (7–37%); c) RNH_2, benzotriazol-1-yloxytripyrrolidinophosphonium hexafluorophosphate, $CHCl_3$ (36–73%); d) $(MeO_2C)_2$, *t*BuOK, DMF, 0 °C→rt, 18 h (96%); e) RNH_2, $AcOH/H_2O$, reflux, 3 h (4–70%).

Of the two sets of analogues, 3-(aminoacetyl)indoles **2** were the more effective antiprion agents, though with much reduced potency compared to their indole-3-glyoxylamide counterparts (Table 2). The indole-3-acetamides **3** performed even more poorly, with only one compound retaining any activity—*p*-morpholinoaniline derivative **3c**, an analogue of the most potent of the parent indole-3-glyoxylamides, **1c**. Thus, both carbonyl groups of the glyoxylamide substructure should be considered essential for the highly potent antiprion activity of indole-3-glyoxylamides **1**, though the carbonyl group adjacent to the indole ring appears to play the more significant role in conferring this effect.

Table 2. Screening results for active compounds from libraries **2** and **3**.

Compd	R	Yield [%][a]	EC_{50}[b] [μM]	EC_{50} (parent)[b,c] [μM]
2a		7	1.40 ± 0.50	0.32 ± 0.02
2b	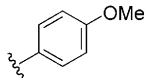	9	0.61 ± 0.45	0.011 ± 0.006
2c	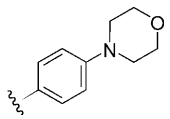	37	0.10 ± 0.02	0.009 ± 0.002
3c	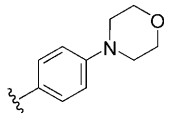	71	3.9 ± 1.9	0.009 ± 0.002

[a] Isolated yield from reaction of **8** with RNH_2 (Scheme 1a; **2a**-**c**), or from coupling of indole-3-acetic acid with *p*-morpholinoaniline (**3c**). [b] Values represent the mean ± SD of at least two experiments, each performed in triplicate. [c] EC_{50} of the analogous indole-3-glyoxylamide compound, as reported previously.[6]

Replacement of the glyoxylamide moiety by a maleimide bridge was also explored (Scheme 1c). Treatment of indole-3-acetamide with dimethyl oxalate under basic conditions provided 3-hydroxymaleimide **9**.[10,11] Subsequent reaction with the same subset of amines employed for libraries **2** and **3**, in refluxing aqueous acetic acid (AcOH),[11] furnished maleimide-bridged analogues **4a**–**d**. However, none of these compounds displayed any efficacy in the SMB assay, underlining the importance of the glyoxylamide moiety to the potent antiprion activity of lead series **1**.

We next looked to prepare analogues incorporating a one- or two-carbon spacer between the glyoxylamide carbonyl groups (Scheme 2). Methylene-bridged compounds **5** were approached by first heating indole with monoethyl malonate in acetic anhydride (Ac_2O) at 85 °C. These conditions were reported for the reaction of indole with cyanoacetic acid, which proceeds in quantitative yield in 30 min;[12] in the present case, a longer reaction time was necessary in order to access the product **10** in acceptable yield. Saponification of **10** was attempted using a procedure reported for basic hydrolysis of the related ethyl 2-(4-methoxybenzoyl)acetate,[13] but the reaction failed, presumably due to ready formation of the enolate of the starting material. Hydrolysis of **10** under acidic conditions (6 M HCl, reflux) only resulted in decomposition, in line with expectations given the reported thermal instability of **12**.[14]

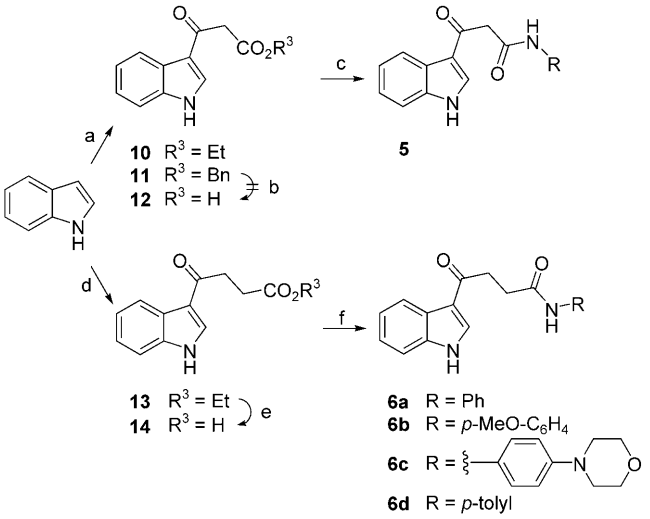

Scheme 2. Approaches to indole-3-glyoxylamide variants incorporating a one or two-carbon spacer. *Reagents and conditions:* a) malonic acid monoester, Ac_2O, 85 °C, 3 h (38%); b) H_2, 10% Pd-C, MeOH, 2 h; c) TBD, RNH_2, 80 °C, 24 h; d) Et_2AlCl, ethyl succinyl chloride, CH_2Cl_2/hexane, 0 °C (42% for step d); e) 2.5% aq KOH, 4 h (54%); f) RNH_2, benzotriazol-1-yl-oxytripyrrolidinophosphonium hexafluorophosphate, iPr_2NEt, $CHCl_3$, RT, 18 h (34–53%).

In the light of these results, direct aminolysis of ester **10** was investigated in a solvent-free procedure mediated by 1,5,7-triazabicyclo[4.4.0]dec-5-ene (TBD).[15] Although this methodology has proven successful in other contexts in our laboratory,[16] none of the desired amide product **5b** was detected upon reaction of **10** with *p*-anisidine under these conditions. As an alternative strategy, reaction of indole with monobenzyl malonate was carried out, successfully resulting in isolation of benzyl ester **11**. Unexpectedly, hydrogenolysis of this intermediate to the free acid failed, instead giving an as yet unidentified product that is not compound **12**. Given the difficulty in obtaining compounds of type **5**, our attention was instead turned towards the synthesis of the two-carbon bridged analogues **6**.

An analogous reaction to the preparation of **10** was attempted, heating indole with monoethyl succinate in Ac_2O, though none of the desired product **13** was observed under these conditions (Scheme 2). Elevation of the temperature resulted only in formation of 3-acetylindole. Intermediate **13** was instead prepared via Friedel–Crafts acylation of indole by ethyl succinyl chloride,[17] and base hydrolysis of the ester then yielded desired acid **14**. Coupling of this intermediate with a small set of amines gave a library of test compounds **6a**–**d**, but none of these compounds demonstrated any antiprion effect in the SMB cell line.

In summary, all attempted modifications to the glyoxylamide substructure proved detrimental to biological activity. Of the

two carbonyl groups, the one directly adjacent to the indole ring at C-3 appears to make the more important contribution to the antiprion activity of the compounds, but the 1,2-dicarbonyl motif is optimal.

Effect of substitution at indole N-1

In our earlier report,[6] it was noted that methyl substitution at indole N-1 raised the EC_{50} value by approximately an order of magnitude, though *N*-methyl analogues of only a small number of active compounds were studied. To improve understanding of the effect of different substituents at this position, a series of *N*-alkylated analogues of present lead **1a** were prepared (Scheme 3).

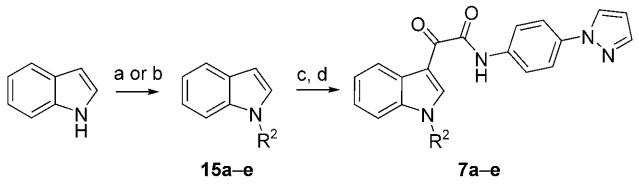

Scheme 3. Preparation of analogues of lead compound **1a** substituted with various groups at indole N-1. *Reagents and conditions:* a) R^2Br or R^2I, *t*BuOK, 18-crown-6, Et_2O, 18 h (22–83%); b) cyclopropylboronic acid, 10 mol% $Cu(OAc)_2$, DMAP, NaHMDS, toluene, dry air, 95 °C, 24 h (39%); c) oxalyl chloride, THF, 1 h; d) *p*-pyrazol-1-ylaniline, 2,6-lutidine, DMAP, 45 °C, 18 h (15–59%, two steps).

The required 1-substituted indoles **15** were synthesised using various alkyl halides in the presence of potassium *tert*-butoxide/18-crown-6,[18] the only exception being 1-cyclopropylindole **15e**, which is not accessible by this method. This intermediate was instead prepared via a copper-catalysed coupling of indole with cyclopropylboronic acid.[19] 1-Alkylindoles **15a–e** were progressed to the desired targets **7a–e** using the established protocol for indole-3-glyoxylamide synthesis.[6]

As is evident from the results of antiprion screening (Table 3), the unsubstituted lead **1a** (where R^2 = H) is the most potent compound, and reduced activity is apparent in all of the N-1 substituted derivatives **7**, qualitatively correlating with the size of the alkyl group introduced at this position. A methyl or ethyl group is tolerated to some extent, but activity tails away sharply with the presence of larger N-1 substituents (**7c–e**).

Table 3. Screening results for 1-substituted indole-3-glyoxylamides **7a–e**.

Compd	R^2	Yield [%][a]	EC_{50}[b] [μM]
1a	H	3[6]	0.0010 ± 0.0004[6]
7a	Me	29	0.0175 ± 0.0002
7b	Et	23	0.097 ± 0.042
7c	*i*Pr	22	0.73 ± 0.06
7d	cyclopropylmethyl	59	0.67 ± 0.30
7e	cyclopropyl	15	1.09 ± 0.16

[a] Isolated yield for synthesis of **7a–e** from **15a–e**. [b] Values represent the mean ± SD of at least two experiments, each performed in triplicate.

Assessment of binding to prion protein

It has been proposed that compounds binding to PrP^C could act as antiprion agents by stabilising the protein in its normal conformation, thereby arresting conversion into the disease-associated isoform, PrP^{Sc}.[20] To ascertain whether the mode of action of the indole-3-glyoxylamides and their analogues might involve such interaction with PrP^C, a surface plasmon resonance (SPR)-based binding assay was carried out, essentially as reported previously.[21]

Interaction with both human (hu-PrP^C) and murine (mo-PrP^C) forms of the protein was assessed. The principle of the assay may be summed up as follows. A solution of each test compound is passed over immobilised protein bound to a sensor chip surface. The SPR response, recorded in the instrument's response units (RU), increases in proportion to any ligand binding that occurs. Results are expressed in a normalised form, $\%RU_{max}$; that is, as a percentage relative to the calculated value of SPR response corresponding to formation of a 1:1 ligand–protein complex. Compounds showing interaction with either form of PrP^C were further characterised by screening over a range of concentrations, to investigate the dose dependence of the observed binding.

Of the present compound libraries, existing lead series **1** showed the lowest levels of affinity for PrP^C, with only **1a** and **1h** demonstrating any significant interaction with the proteins. The observed binding appeared to be rather weak, however, with the SPR response falling well below the level expected for 1:1 complex formation, even at a ligand concentration of 100 μM (Figure 5a; data shown for **1a**). In contrast, maleimide-bridged analogues **4a–d** all showed good binding to PrP^C, despite their lack of antiprion activity. However, the linear dose–response relationship seen for these compounds strongly suggests a nonspecific binding interaction with hu-PrP^C (Figure 5b).

The results of most initial interest were obtained for 3-(aminoacetyl)indole family **2a–d** (Figure 5c), with compounds **2a** (Scheme 1a; R = Ph) and **2c** (R = *p*-morpholinophenyl) in particular showing strong affinity for both forms of PrP^C. As concentration is increased, the approach of SPR response towards a limiting value is suggestive of a specific interaction with the proteins; namely, formation of a 2:1 ligand–protein complex in the case of **2a**, and a 1:1 complex for **2c** (with observed K_D = 53 ± 6 μM for hu-PrP^C, and 85 ± 24 μM for mo-PrP^C). Sensorgrams obtained during evaluation of **2a** clearly illustrate the upward trend in SPR response as ligand concentration is increased (Figure 5d). Closely related structures **2b** (R = *p*-methoxyphenyl) and **2d** (R = benzyl) exhibited significantly weaker, and apparently nonspecific, binding (Figure 2c).

All compounds showing evidence of binding to PrP^C were assessed for their tendency to form aggregates in aqueous solution, using the dynamic light scattering (DLS) technique. In recent years, aggregation-based effects have increasingly been acknowledged as a major source of 'false positive' hits in protein binding or enzyme inhibition assays.[22] Thus, it is important to be aware that larger particles formed via aggregation of small organic molecules may sequester protein and lead to

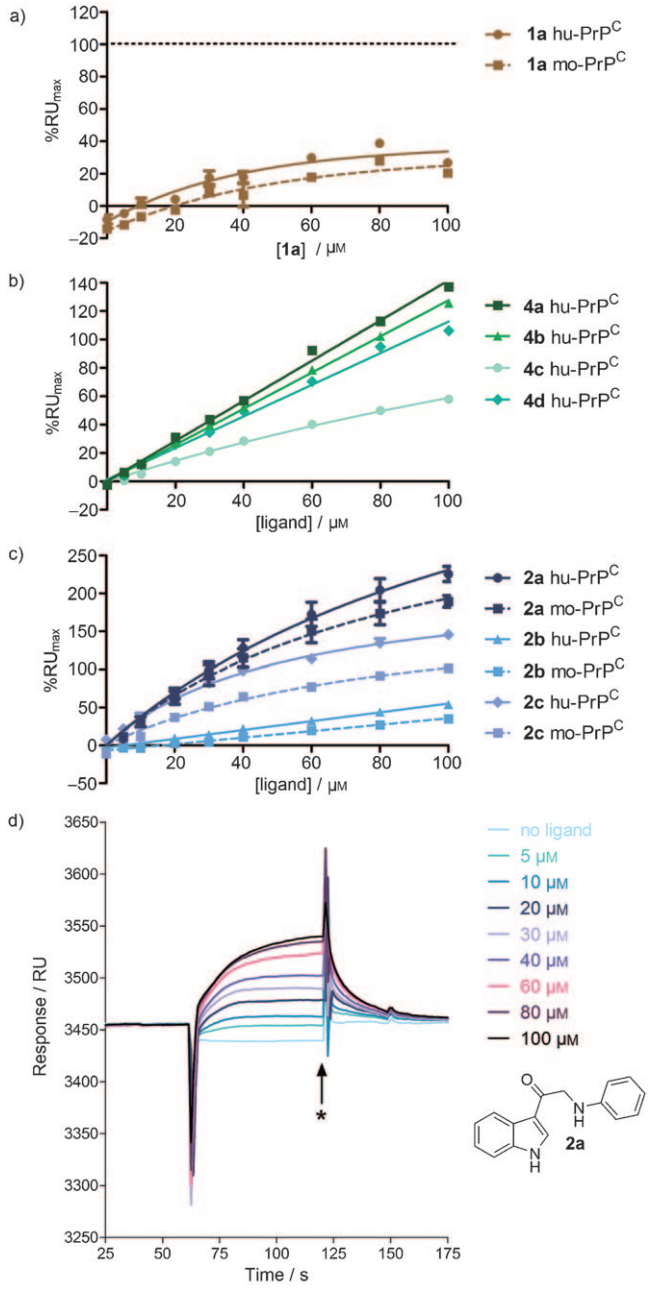

Figure 5. Binding of indole-based screening compounds to immobilised human (hu-PrP^C) and murine (mo-PrP^C) forms of recombinant prion protein, as evaluated by surface plasmon resonance (SPR). a) Nanomolar-active antiprion compound **1a** showed only a weak interaction with PrP^C (----- represents the theoretical response for 1:1 binding); b) Maleimide-bridged analogues **4a**–**d** all displayed binding to hu-PrP^C, although the linear dose–response relationship suggests that this observed binding is nonspecific in nature. Data for the murine protein were similar and are presented in the Supporting Information; c) The 3-(aminoacetyl)indoles **2a**–**d** also gave positive results; data for **2d** are omitted for clarity but are similar to those for **2b**; d) Example sensorgrams obtained during evaluation of **2a** at varying concentration, showing association and dissociation phases of the binding event. An asterisk denotes the point at which binding levels (%RU$_{max}$) are recorded, at the end of the association phase.

a mistaken impression of binding. Secondary assays to further characterise any apparent ligands for a protein of interest are therefore desirable to discern between true and false positive results.

Of the present test compounds, **1a** was found to form detectable particles of approximately 200 nm diameter, even at low concentrations (0.1–5 μM); at 10 μM, larger aggregates exceeding 1 μm in diameter were identified. The weak interaction of **1a** with PrP^C observed by SPR (Figure 5a) may thus be assumed to reflect interaction of the protein with the formed aggregates, rather than true ligand binding. Indeed, the type of substoichiometric binding seen for **1a** was found to be one characteristic of aggregation behaviour in a recent study investigating the SPR behaviour of known aggregators.[23]

The same report also identified superstoichiometric effects as a signature of aggregates, in the light of which it was unsurprising to discern putative 2:1 binder **2a** as a strong aggregator (Figure 6a), which forms large particles over the concentration range studied in the SPR assay. The noted approach of SPR response towards a limiting value (Figure 5c) must likely represent the covering of the available protein surface by these sizeable aggregates, with the same being true for **2c**. Indeed, since the general aggregation tendency of family **2a**–**d** (**2a** ≈ **2c** ⩾ **2b** ≈ **2d**; Figure 6a) so closely matches the observed PrP^C binding affinities, it may be concluded that this group of compounds do not act as genuine ligands for the protein.

In contrast, maleimide-bridged series **4a**–**d** displayed considerably lower aggregation tendency (Figure 6b)—particularly **4a** (R = Ph) and **4d** (R = Bn), which both showed a negligible propensity to aggregate. For these two analogues in particular, the SPR results indicate a definite interaction with both forms of PrP^C, although as already commented, the observed linear dose–response relationship (Figure 5b) is characteristic of nonspecific or promiscuous protein binding.

In summary, none of the cell-line active indole compounds reported herein were found to bind to human or murine prion protein, making it apparent that the antiprion effect of the indole-3-glyoxylamide (and related) libraries does not stem from any direct interaction with PrP^C itself.

Validation of lead-like properties of the glyoxylamide series

In order to evaluate the preclinical potential of glyoxylamide series **1**, a long-term assessment of PrP^{Sc} levels in treated SMB cells was undertaken. After a single treatment with **1a**, cells were passaged and analysed repeatedly every 4–5 days to look for any recovery in PrP^{Sc} levels over time. It was pleasing to find that a single dose of **1a** (at 10 nM) seemed to cure the infected cells indefinitely, with no reappearance of PrP^{Sc} for the full duration of the assay, up to 76 days post treatment (Figure 7). Administering **1a** at its EC$_{50}$ concentration of 1 nM gave only partial reduction in PrP^{Sc} levels, as might reasonably be expected. Cells dosed with quinacrine (EC$_{50}$ = 0.42 μM[6]) as a positive control, at either 1 μM or 5 μM, were also cured for as long as could be assessed, with a large reduction (~80%) in PrP^{Sc} at 1 μM and complete elimination of the disease-associated protein at 5 μM. Barret et al. noted reappearance of PrP^{Sc} in quinacrine-treated ScGT1 cells beginning after 15 passages,[24]

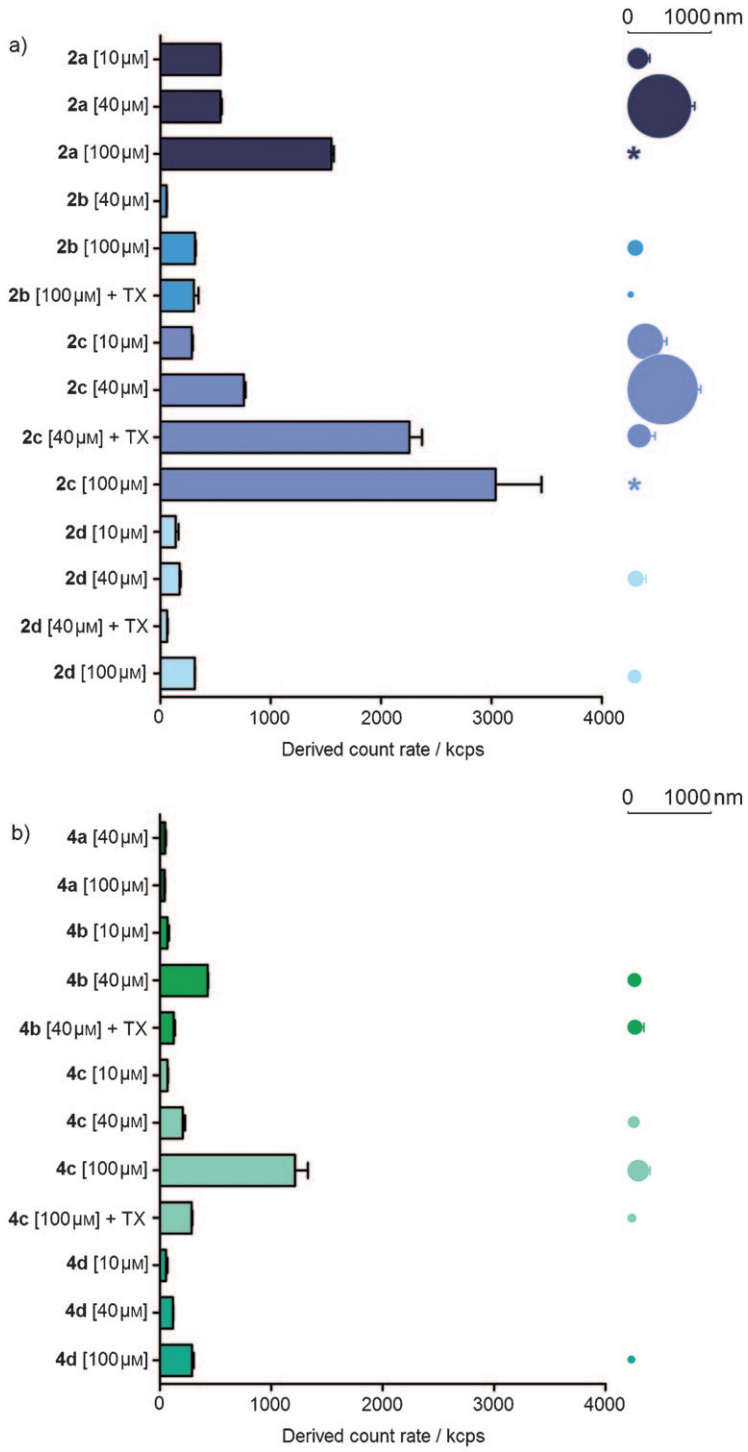

Figure 6. Results of dynamic light scattering (DLS) experiments on a) compounds **2a–d** and b) compounds **4a–d**. A high count rate indicates increasing presence of light-scattering particles in solution. Where particles were detected, their size is represented to scale to the right hand side of the bar chart, with an asterisk denoting the presence of particles >1 μm in diameter. 'TX' denotes the presence of Triton X-100, a non-ionic detergent, at 0.01% *v/v*, which serves to break up and/or arrest the formation of aggregates. All experiments were conducted in 50 mM potassium phosphate buffer, pH 7.4. Benzyl benzoate (250 μM) was employed as a positive control, forming particles of 540 ± 25 nm diameter under the assay conditions.

though no such effect was evident in the present study. Evaluation of the cured SMB cells for longer than the 16 passages shown was not possible however, since they do not seem as robust as other cell lines. Cells must be split promptly upon reaching confluence, and become fatigued with repeated passaging such that division and proliferation become appreciably slower. Nevertheless, in the long-term experiment described (Figure 7), lead compound **1a** was demonstrated to cure a scrapie-infected cell line at concentrations an impressive three orders of magnitude below those required for quinacrine; the drug which has been most thoroughly investigated in both animal[24,25] and clinical[26] prion disease, albeit with minimal success.

In addition to demonstrable potency in a relevant disease model, other properties are important when judging lead-likeness of a compound series. Two such parameters were considered for the present libraries: lipophilicity and stability to a mouse liver microsome (MLM) preparation, as a primary screen to assess likelihood of significant first-pass metabolism.

The effect of lipophilicity upon antiprion activity has already been described for the indole series (Figure 4b), but in the present context, it is important to note that recent analyses[27] have indicated quite a narrow optimal window of log *D* values for successful drugs, typically in the range 1.0–3.0. It was therefore pleasing to confirm that for the large majority of highly potent compounds ($EC_{50} < 20$ nM), clog *D* at neutral pH lies within or only just outside these limits (Table 4). Of particular interest are *p*-(1,3,4-oxadiazol-2-yl) derivative **1m** and *p*-(1*H*-imidazol-1-yl) analogue **1h**, both of which possess clog $D < 2$ and an antiprion EC_{50} value in the order of 1 nM.

Selected members of the screening libraries were further scrutinised by examining their stability towards a mouse liver microsome (MLM) preparation. Simple assessment of the amount of compound remaining following a 30 min incubation is an assay commonly employed during early stage drug discovery, to filter out any especially metabolically labile compounds. Pleasingly, structures of type **1** largely proved robust towards microsomal metabolism over this timescale (Table 4), the only exception being 3,5-dimethyl-1*H*-pyrazol-1-yl analogue **1i**. Existing lead **1a** remained intact when the assay duration was extended from 30 min to 120 min (89.9 ± 3.9% remaining), indicating a half life of several hours with respect to microsomal metabolism. In contrast, 1-alkylindole series **7** was considerably less stable, with only 1-isopropyl and 1-(cyclopropyl)methyl derivatives **7c** and **7d** remaining largely unaffected. The most potent antiprion agents within this series, *N*-methyl and *N*-ethyl analogues **7a** and **7b**, were unsurprisingly metabolised rather rapidly.

As alluded to earlier, the most active compounds of type **1**, which bear a heteroaromatic substituent at the *p*-position of the aniline ring, tend to possess poor solubility relative to other, nonaromatic substituted analogues (e.g.,

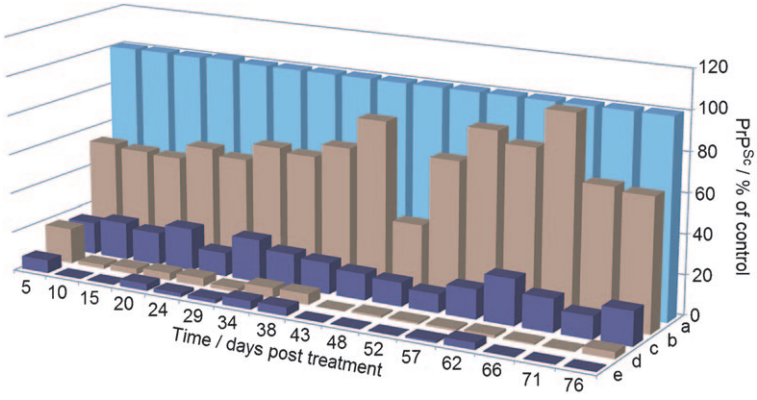

Figure 7. Assessment of antiprion effect of **1a** and quinacrine over multiple passages, following application of a single initial dose to the cells. Major horizontal axis represents time in days post treatment; minor axis identifies data sets a–e; vertical axis shows PrP^{Sc} as a percentage of the control. Bar heights correspond to the PrP^{Sc} level recorded for each passage of the following experiments: a) untreated control; b) dosed with **1a** at 1 nM; c) quinacrine at 1 μM; d) **1a** at 10 nM; e) quinacrine at 5 μM.

Table 4. Cell line antiprion potency, calculated octanol/buffer distribution coefficient (clog *D*), and stability to a mouse liver microsome (MLM) preparation of selected compounds from the indole-3-glyoxylamide lead series.

Compd	EC_{50}[a] [nM]	clog *D*[b]	MLM stability[c] [%]
1a	1.0 ± 0.4	3.11	93.6 ± 4.7
1m	1.1 ± 0.2	1.95	90.4 ± 7.1
1h	1.3 ± 0.2	1.90	92.3 ± 1.3
1g	4.3 ± 0.8	2.42	90.6 ± 1.8
1j	4.4 ± 2.8	3.48	96.4 ± 0.9
1b	6 ± 3	3.24	93.6 ± 9.2
7a	17.5 ± 2.0	3.33	61.1 ± 0.6
1e	19 ± 5	2.53	73.7 ± 3.4
1o	21 ± 4	3.73	88.0 ± 4.2
7b	97 ± 42	3.69	50.4 ± 2.2
1i	109 ± 65	3.44	43.3 ± 5.6
1k	125 ± 21	3.54	87.1 ± 0.7
7d	670 ± 300	4.11	84.3 ± 3.0
7c	730 ± 60	4.11	81.8 ± 1.8
7e	1090 ± 160	3.80	55.6 ± 4.7

[a] Values represent the mean ± SD of at least two experiments, each performed in triplicate. [b] clog *D* values quoted for pH 7.4. These data were calculated using a clog *P*/clog *D* calculator available online.[8] [c] Percentage of compound remaining after 30 min incubation with mouse liver microsome (MLM) preparation.

1d and **1k**). Although the former are active at very low concentrations, making low solubility less problematic, it would nonetheless be desirable to improve this property of the most potent leads.

Conclusion

The structure–activity relationships of indole-3-glyoxylamide series **1** as potent antiprion compounds have been further refined, revealing five-membered heterocycles as optimal substituents at the key *p*-position of the aniline ring (R^1; Figure 1). It seems apparent that the heterocyclic moiety should ideally contain at least two heteroatoms. A number of modifications to the glyoxylamide substructure were carried out in an attempt to improve potency but proved unfruitful, with all changes to the structure resulting in compounds with lower or no antiprion activity. Probing the effect of substitution at indole N-1 gave similar results.

No cell-line active compounds within the present study demonstrated any discernible, genuine binding to prion protein, indicating that the biological activity of lead series **1** is not mediated through direct interaction with PrP^C. Further investigations are evidently necessary to elucidate the mode of action of these highly potent antiprion agents.

The most potent structures of type **1** showed good lead-like properties, possessing suitably low clog *D* and good resistance towards microsomal metabolism, in addition to EC_{50} values in the low nanomolar range (seven examples <10 nM). A single treatment with **1a** cured prion-infected cells over multiple passages. Of all the compounds screened herein, only one (**1p**) was found to exert a cytotoxic effect upon the SMB cells at concentrations up to 20 μM. Thus, the indole-3-glyoxylamide compounds reported herein merit continued in vitro and in vivo evaluation as potential therapeutics for human prion diseases.

Experimental Section

Materials and general methods: Anhydrous tetrahydrofuran (THF), Et_2O, CH_2Cl_2 and toluene were obtained from an in-house Grubbs apparatus. Reagents for SPR screening: *N*-hydroxysuccinimide, *N*-ethyl-*N*′-(3-diethylaminopropyl)carbodiimide hydrochloride (EDC), 1 M ethanolamine, HBS-EP buffer, surfactant P20, regeneration solution (10 mM glycine–HCl pH 3.0) and CM-dextran (MW = 13 kDa), were all purchased from GE Healthcare Bio-Sciences AB (Uppsala, Sweden). Recombinant full-length human prion protein (hu-PrP^C) and full-length mouse prion protein (mo-PrP^C) were generous gifts from Dr. Andrew Gill (Roslin Institute, University of Edinburgh, UK). All other reagents and solvents were obtained from appropriate commercial sources and used as supplied. Parallel synthesis was carried out on a Radleys 12-position carousel in 50 mL boiling tubes. Melting points were determined using a Gallenkamp melting point apparatus in capillary tubes and are uncorrected. ^1H and ^{13}C NMR spectra were recorded at 400 MHz and 100 Hz, respectively, on a Bruker AV-1400 spectrometer; or at 250 MHz and 62.8 MHz, respectively, on a Bruker AV-1250 model. Mass spectra were acquired using a Micromass LCT Premier XE system. Infrared spectra were recorded on a Perkin–Elmer Spectrum RX machine fitted with a SensIR Technologies Durasampl*IR* II device. Dynamic light scattering (DLS) measurements were carried out using a Malvern Instruments Zetasizer Nano ZS system, equipped with a 4 mW He-Ne laser at 633 nm. HPLC analysis was carried out using a Genesis 4 μm C18 column (4.6 × 150 mm) eluted with a gradient of MeCN/H_2O (30 → 100% over 12 min; hold at 100% MeCN for 10 min), flow rate 1 mL min^{-1}, with UV detection at 254 nm.

Biology

Assessment of antiprion activity in SMB cells: Compounds were screened for inhibition of PrP^{Sc} formation in SMB cells of mesodermal origin (SMB.s15 cell line[5]) as described previously.[6] Cells were grown in tissue-culture-treated plastic dishes in Medium 199 (phenol-red free), supplemented with 10% newborn calf serum (heat inactivated), 5% fetal calf serum (heat inactivated), and penicillin–streptomycin at 10 mg L^{-1} at 37 °C in an atmosphere of 5% CO_2 in air at 95% relative humidity. Medium was changed every third or fourth day, and every seven days confluent cells were passaged using 0.05% trypsin and 0.002% EDTA at a split ratio of four. To assess the effects of compounds, cells were distributed into 96-well cluster plates at 3×10^4 cells per well and incubated for 24 h to allow for cell attachment. The compounds were prepared at 400 times the required concentration in DMSO as stock solutions then transferred, at a 20-fold dilution, into Hank's balanced salt solution. This solution was then transferred at a further 20-fold dilution into the cell medium. The cells were incubated with the compound-containing medium for five days. After this time, cell viability was assessed by the MTT assay following the standard protocol supplied with the reagent (Sigma).

For dot blot (cell blot) analyses, cells were extracted using lysis buffer (10 mM Tris-HCl (pH 7.6), 100 mM NaCl, 10 mM EDTA, 0.5% *v/v* NP40, and 0.5% *w/v* sodium deoxycholate), and the content of the well was loaded onto a nitrocellulose membrane (0.45 μm) under gentle vacuum at a total cellular protein concentration of approximately 30–40 μg per well (determined by the Bradford assay following the protocol supplied with the reagent; Sigma). The membrane was air dried and subjected to 75 μg mL^{-1} proteinase K digestion for 1 h at 37 °C. The reaction was stopped with 1 mM phenylmethylsulfonyl fluoride (PMSF) in 20 mM Tris-HCl-buffered saline (TBS) and the membrane washed extensively with TBS and immersed in 1.8 M guanidine thiocyanate in TBS for 10 min at RT. After further washing with TBS, the membrane was blocked using 5% fat-free milk powder in phosphate-buffered saline (PBS), processed with 0.2 μg mL^{-1} mouse monoclonal antiPrP 6H4 (Prionics; Zürich, Switzerland), and developed using an ECL kit (Amersham Pharmacia Biotech). Every experiment was carried out in triplicate and an average value for PrP^{Sc} concentration calculated, relative to an untreated control (DMSO only), together with a standard deviation (SD). Curcumin was employed as a positive control, and effected essentially complete clearance of PrP^{Sc} at the concentration used (10 μM). Test compounds were initially screened at 1, 10 and 20 μM and were considered to be active if PrP^{Sc} levels were reduced to less than 70% of that of the untreated control after exposure for five days. Compounds showing activity were rescreened over a range of concentrations to determine an EC_{50} value, such experiments being repeated at least twice (in triplicate) to validate the results so obtained. Screening in the SMB.s15 line was previously validated by investigating two well-documented antiprion agents as positive controls.[6] EC_{50} values of 0.95 μM and 0.42 μM were observed for curcumin and quinacrine, respectively, in this cell line.

Assessment of binding to PrP^C via SPR: The method used was essentially as reported previously.[16,21] Experiments were carried out using a Biacore 3000 instrument equipped with a CM5 sensor chip, containing a CM-dextran surface. Prior to screening, PrP^C was immobilised on the chip surface according to the following protocol: A 1:1 mixture of 100 mM *N*-hydroxysuccinimide and 400 mM EDC was passed over the sensor chip for 7 min at a flow rate of 5 μL min^{-1}. A solution of PrP^C, at a concentration of 2 μg mL^{-1} in HBS-EP buffer, was then passed over the chip surface for 7 min. Unreacted sites were blocked by injection of 1 M ethanolamine, pH 8.5, for 7 min, after which the chip surface was prepared for use by three consecutive injections (5 μL at 30 μL min^{-1}) of 25 mM NaOH/1 M NaCl solution. Finally, the sensor chip surface was equilibrated with running buffer (10 mM Na_3PO_4, pH 7.4; 150 mM NaCl; 3.4 mM EDTA; 0.005% *v/v* surfactant P20) overnight prior to screening. The four flow cells of the Biacore instrument were employed as follows: flow cell 1 was used as a reference surface (no immobilised protein); flow cells 2 and 4 contained hu-PrP^C; and flow cell 3 contained mo-PrP^C. Test compounds were dissolved in DMSO at 800 μM and diluted to the required concentration (40 μM for routine screening; variable concentrations for K_d determination) using running buffer, prior to injection. Assays were performed at 25 °C with a flow rate of 30 μL min^{-1}. To correct for solvent effects, 6.5% DMSO was added to the running buffer, and DMSO calibration sequences using buffer samples containing 5.5–7.5% DMSO (in 0.5% intervals) were carried out at the start of each run, and after every 10 test compounds. Each analytical cycle consisted of running buffer for 1 min (stabilisation phase), sample injection for 1 min (association phase), and running buffer for 3 min (dissociation phase). Between cycles, surface regeneration was carried out at 35 μL min^{-1} by injecting 25 mM NaOH/1 M NaCl/0.0005% SDS pH 8.5 (for 30 s), then by 10 mM glycine–HCl pH 3.0 (for 35 s), followed by a re-equilibration phase in running buffer for 1 min. Each test compound was injected in triplicate in order to establish an average response (recorded in resonance units, RU) and a standard deviation (SD). Binding affinities are expressed as $\%RU_{max}$, where RU_{max} is the theoretical response for a 1:1 binding interaction between the ligand and PrP^C, calculated according to Equation (1), where $RU_{immobilised\ protein}$ is the response (in RU) seen at the end of the immobilization procedure.

$$RU_{max} = (RU_{immobilised\ protein}/MW_{protein}) \times MW_{ligand} \quad (1)$$

Microsomal stability assay: The procedure was modified from that reported in a recent study of quinacrine metabolism.[28] A mixture of test compound (5.0 mM stock solution in DMSO; 0.8 μL), isocitrate dehydrogenase (31.4 μL, 2 units), 0.2 M potassium phosphate buffer (pH 7.0, containing 10 mM DL-isocitric acid trisodium salt and 10 mM $MgCl_2$; 228 μL), and microsome preparation from mouse liver (0.5 mg mL^{-1} in the same buffer; 100 μL) was incubated in an Eppendorf tube for 5 min at 37 °C. NADPH (10 mM stock solution; 40 μL) was then added to initiate the reaction. The contents of the tube were mixed using aspiration/dispensation five times, then a $t=0$ aliquot (150 μL) was drawn immediately and quenched with ice-cold acetonitrile (300 μL), containing 8 μM 1-(2-methyl-1*H*-indol-3-yl)-2-morpholinoethane-1,2-dione[6] as internal reference standard. The remaining reaction mixture was maintained at 37 °C for 30 min, then a second aliquot removed and diluted as above. The quenched solutions were each vortexed for 30 s and centrifuged at 4000 rpm for 10 min, then the supernatant analysed by HPLC: Genesis 4 μm C18 column, 4.6×150 mm; 5–95% MeCN/H_2O over 4 min, hold 6 min at 95% MeCN; flow rate 1 mL min^{-1}; UV detection at 267 nm. Each analysis was performed in triplicate and metabolism results after 30 min compared with those at $t=0$. The percentage of drug remaining, together with the standard deviation (SD), is reported for each test compound.

Chemistry

Assessment of aggregation tendency by dynamic light scattering (DLS): Compounds were diluted from a 10 mM DMSO stock solution to the required concentration in 50 mM potassium phos-

phate buffer, pH 7.4 (0.2 μm prefiltered), at a final DMSO concentration of 2%. Three measurements of the derived count rate (in kilocounts per second; kcps) were taken, and a mean value is reported for each sample assessed, together with the standard deviation over the three results. Data collection and quality assessment were carried out using the software supplied with the instrument (Dispersion Technology Software, v. 5.03, Malvern Instruments).

General synthesis of indole-3-glyoxylamides (1g–p, 7a–e): Indole or *N*-alkylindole (1.5 mmol), as appropriate, was dissolved in dry THF (15 mL) under N_2. Oxalyl chloride (144 μL, 209 mg, 1.65 mmol) was added, and the solution stirred at RT for 60 min. 2,6-Lutidine (408 μL, 375 mg, 3.5 mmol) was then introduced to the reaction mixture, followed by the relevant *p*-substituted aniline (1.8 mmol), and DMAP (catalytic amount). The reaction mixture was warmed to 45 °C and heated with rapid stirring for 18 h. The crude reaction was then concentrated, and the residue was suspended in warm EtOAc (25 mL) and stirred vigorously with brine (15 mL) for 10–15 min. The mixture was separated using a liquid–liquid extraction column (20 mL capacity), and the column was washed through with additional EtOAc to ensure optimum recovery. A second extraction with saturated aq NH_4Cl (15 mL) was carried out in the same manner, and the resultant solution evaporated providing the crude product. Two sequential recrystallisations, first from EtOAc/hexane, then from 2-propanol/water, were performed, and these typically provided products of good purity (>95% by HPLC).

***N*-(4-(1*H*-1,2,4-Triazol-1-yl)phenyl)-2-(1*H*-indol-3-yl)-2-oxoacetamide (1g)**: Pale yellow solid (29 mg, 6%): ^{1}H NMR (400 MHz, [D$_6$]DMSO): δ = 12.39 (s, 1H), 10.95 (s, 1H), 9.28 (s, 1H), 8.81 (s, 1H), 8.34–8.28 (m, 1H), 8.25 (s, 1H), 8.07 (d, J = 9.5 Hz, 2H), 7.89 (d, J = 9.0 Hz, 2H), 7.60–7.55 (m, 1H), 7.34–7.28 ppm (m, 2H); ^{13}C NMR (100 MHz, [D$_6$]DMSO): δ = 111.9, 112.7, 119.9, 121.1, 121.2, 122.8, 123.6, 126.2, 132.8, 136.4, 137.6, 138.7, 142.1, 152.3, 162.4, 181.6 ppm; IR (solid): $\tilde{\nu}$ = 3318, 3119, 1674, 1625, 1596, 1529, 1493, 1429, 1275, 1240, 1123, 833, 787, 742, 672, 648 cm^{-1}; MS (ES): *m/z* (%): 332 (100) $[M+H]^+$; HRMS-ES: *m/z* $[M+H]^+$ calcd for $C_{18}H_{15}N_5O_2$: 332.1147, found: 332.1132.

***N*-(4-(1*H*-Imidazol-1-yl)phenyl)-2-(1*H*-indol-3-yl)-2-oxoacetamide (1h)**: Pale brown needles (21 mg, 3%): ^{1}H NMR (400 MHz, [D$_6$]DMSO): δ = 12.38 (s, 1H), 10.89 (s, 1H), 8.80 (s, 1H), 8.33–8.27 (m, 1H), 8.26 (s, 1H), 8.02 (d, J = 9.0 Hz, 2H), 7.75 (s, 1H), 7.69 (d, J = 9.5 Hz, 2H), 7.60–7.55 (m, 1H), 7.34–7.28 (m, 2H), 7.12 ppm (s, 1H); ^{13}C NMR (100 MHz, [D$_6$]DMSO): δ = 111.9, 112.7, 118.0, 120.7, 121.2, 121.3, 122.7, 123.6, 126.2, 129.8, 133.0, 135.4, 136.4, 136.7, 138.7, 162.3, 181.6 ppm; IR (solid): $\tilde{\nu}$ = 3333, 1691, 1626, 1521, 1450, 1306, 1241, 1113, 1062, 922, 832, 785, 740, 679, 650, 619 cm^{-1}; MS (ES): *m/z* (%): 331 (100) $[M+H]^+$; HRMS-ES: *m/z* $[M+H]^+$ calcd for $C_{19}H_{15}N_4O_2$: 331.1195, found: 331.1205.

***N*-(4-(3,5-Dimethyl-1*H*-pyrazol-1-yl)phenyl)-2-(1*H*-indol-3-yl)-2-oxoacetamide (1i)**: Microcrystalline, pale brown solid (322 mg, 45%): ^{1}H NMR (400 MHz, [D$_6$]DMSO): δ = 12.38 (s, 1H), 10.89 (s, 1H), 8.80 (s, 1H), 8.34–8.28 (m, 1H), 8.00 (d, J = 9.0 Hz, 2H), 7.61–7.55 (m, 1H), 7.50 (d, J = 9.0 Hz, 2H), 7.34–7.28 (m, 2H), 6.06 (s, 1H), 2.30 (s, 3H), 2.19 ppm (s, 3H); ^{13}C NMR (100 MHz, [D$_6$]DMSO): δ = 12.1, 13.3, 106.9, 111.9, 112.7, 120.6, 121.2, 122.7, 123.6, 124.5, 126.2, 135.6, 136.4, 136.8, 138.6, 139.0, 147.6, 162.4, 181.8 ppm; IR (solid): $\tilde{\nu}$ = 3349, 3165, 3064, 2924, 1688, 1629, 1504, 1443, 1411, 1126, 844, 783, 741, 664, 612 cm^{-1}; MS (ES): *m/z* (%): 359 (100) $[M+H]^+$; HRMS-ES: *m/z* $[M+H]^+$ calcd for $C_{21}H_{19}N_4O_2$: 359.1508, found: 359.1515.

2-(1*H*-Indol-3-yl)-*N*-(4-(1-methyl-1*H*-pyrazol-3-yl)phenyl)-2-oxoacetamide (1j): Pale yellow powder (14 mg, 3%): ^{1}H NMR (400 MHz, [D$_6$]DMSO): δ = 12.37 (s, 1H), 10.75 (s, 1H), 8.79 (s, 1H), 8.33–8.27 (m, 1H), 7.90 (d, J = 8.5 Hz, 2H), 7.79 (d, J = 8.5 Hz, 2H), 7.73 (d, J = 2.0 Hz, 1H), 7.60–7.54 (m, 1H), 7.33–7.28 (m, 2H), 6.68 (d, J = 2.0 Hz, 1H), 3.89 ppm (s, 3H); ^{13}C NMR (100 MHz, [D$_6$]DMSO): δ = 38.6, 102.3, 111.9, 112.6, 120.3, 121.2, 122.7, 123.6, 125.3, 126.2, 129.6, 132.2, 136.4, 137.2, 138.6, 149.6, 162.2, 181.9 ppm; IR (solid): $\tilde{\nu}$ = 3347, 3167, 3046, 2926, 1682, 1626, 1488, 1427, 1309, 1244, 1129, 948, 842, 786, 744, 680, 652 cm^{-1}; MS (ES): *m/z* (%): 345 (100) $[M+H]^+$; HRMS-ES: *m/z* $[M+H]^+$ calcd for $C_{20}H_{17}N_4O_2$: 345.1352, found: 345.1355.

2-(1*H*-Indol-3-yl)-2-oxo-*N*-(4-(pyrrolidin-1-yl)phenyl)acetamide (1k): Bright orange solid (81 mg, 16%): ^{1}H NMR (400 MHz, [D$_6$]DMSO): δ = 12.31 (s, 1H), 10.36 (s, 1H), 8.82 (s, 1H), 8.33–8.27 (m, 1H), 7.69 (d, J = 8.5 Hz, 2H), 7.60–7.53 (m, 1H), 7.33–7.26 (m, 2H), 6.54 (d, J = 9.5 Hz, 2H), 3.21 (t, J = 6.0 Hz, 4H), 1.95 ppm (t, J = 6.0 Hz, 4H); ^{13}C NMR (100 MHz, [D$_6$]DMSO): δ = 24.9, 47.4, 111.3, 112.1, 112.6, 121.2, 121.6, 122.6, 123.4, 126.3, 126.7, 136.3, 138.5, 144.9, 161.3, 182.3 ppm; IR (solid): $\tilde{\nu}$ = 3298, 2970, 2847, 1672, 1611, 1516, 1501, 1438, 1369, 1107, 964, 812, 740, 682, 657 cm^{-1}; MS (ES): *m/z* (%): 334 (100) $[M+H]^+$; HRMS-ES: *m/z* $[M+H]^+$ calcd for $C_{20}H_{20}N_3O_2$: 334.1556, found: 334.1567.

***N*-(4-((1*H*-Pyrazol-1-yl)methyl)phenyl)-2-(1*H*-indol-3-yl)-2-oxoacetamide (1l)**: Pale yellow powder (217 mg, 42%): ^{1}H NMR (400 MHz, [D$_6$]DMSO): δ = 12.35 (s, 1H), 10.72 (s, 1H), 8.76 (s, 1H), 8.32–8.25 (m, 1H), 7.87–7.78 (m, 3H), 7.60–7.54 (m, 1H), 7.49–7.46 (br s, 1H), 7.33–7.21 (m, 4H), 6.28 (t, J = 2.0 Hz, 1H), 5.32 ppm (s, 2H); ^{13}C NMR (100 MHz, [D$_6$]DMSO): δ = 55.1, 106.3, 112.8, 113.6, 121.2, 122.1, 123.6, 124.5, 127.0, 129.0, 130.8, 134.4, 137.2, 138.3, 139.5, 139.8, 163.2, 182.7 ppm; IR (solid): $\tilde{\nu}$ = 3342, 3150, 3112, 2934, 1691, 1629, 1530, 1492, 1446, 1414, 1244, 1128, 737, 688 cm^{-1}; MS (ES): *m/z* (%): 345 (100) $[M+H]^+$; HRMS-ES: *m/z* $[M+H]^+$ calcd for $C_{20}H_{17}N_4O_2$: 345.1352, found: 345.1348.

***N*-(4-(1,3,4-Oxadiazol-2-yl)phenyl)-2-(1*H*-indol-3-yl)-2-oxoacetamide (1m)**: Pale orange powder (20 mg, 4%): ^{1}H NMR (400 MHz, [D$_6$]DMSO): δ = 12.41 (s, 1H), 11.08 (s, 1H), 9.34 (s, 1H), 8.78 (d, J = 3.0 Hz, 1H), 8.34–8.26 (m, 1H), 8.12 (d, J = 9.0 Hz, 2H), 8.06 (d, J = 8.5 Hz, 2H), 7.61–7.54 (m, 1H), 7.36–7.27 ppm (m, 2H); ^{13}C NMR (100 MHz, [D$_6$]DMSO): δ = 112.7, 113.6, 119.5, 121.5, 122.1, 123.7, 124.5, 127.0, 128.5, 137.3, 139.6, 142.3, 155.2, 163.6, 164.3, 182.3 ppm; IR (solid): $\tilde{\nu}$ = 3321, 3149, 3103, 1692, 1611, 1590, 1509, 1487, 1447, 1415, 1242, 1140, 1103, 1076, 785, 738, 642 cm^{-1}; MS (ES): *m/z* (%): 333 (100) $[M+H]^+$; HRMS-ES: *m/z* $[M+H]^+$ calcd for $C_{18}H_{13}N_4O_3$: 333.0988, found: 333.1003.

***N*-(4-(2-Cyclopropyloxazol-5-yl)phenyl)-2-(1*H*-indol-3-yl)-2-oxoacetamide (1n)**: Golden brown needles (78 mg, 14%): ^{1}H NMR (400 MHz, [D$_6$]DMSO): δ = 12.38 (s, 1H), 10.85 (s, 1H), 8.80 (d, J = 3.0 Hz, 1H), 8.33–8.27 (m, 1H), 7.97 (d, J = 9.0 Hz, 2H), 7.67 (d, J = 9.0 Hz, 2H), 7.60–7.55 (m, 1H), 7.45 (s, 1H), 7.34–7.27 (m, 2H), 2.21–2.12 (m, 1H), 1.11–0.99 ppm (m, 4H); ^{13}C NMR (100 MHz, [D$_6$]DMSO): δ = 8.0, 8.5, 111.9, 112.7, 120.5, 121.2, 121.9, 122.7, 123.6, 124.1, 126.2, 136.4, 137.8, 138.6, 149.4, 162.3, 164.8, 181.6 ppm; IR (solid): $\tilde{\nu}$ = 3316, 3056, 1678, 1575, 1508, 1492, 1442, 1415, 1119, 813, 784, 730, 685, 658 cm^{-1}; MS (ES): *m/z* (%): 372 (100) $[M+H]^+$; HRMS-ES: *m/z* $[M+H]^+$ calcd for $C_{22}H_{18}N_3O_3$: 372.1348, found: 372.1355.

***N*-(4-(Furan-2-yl)phenyl)-2-(1*H*-indol-3-yl)-2-oxoacetamide (1o)**: Microcrystalline, yellow solid (150 mg, 23%): ^{1}H NMR (400 MHz, [D$_6$]DMSO): δ = 12.37 (s, 1H), 10.82 (s, 1H), 8.80 (d, J = 3.5 Hz, 1H), 8.34–8.27 (m, 1H), 7.95 (d, J = 9.0 Hz, 2H), 7.76–7.70 (m, 3H), 7.60–

7.54 (m, 1H), 7.34–7.28 (m, 2H), 6.91 (d, J=3.0 Hz, 1H), 6.60 ppm (dd, J=2.0 Hz, 3.5 Hz, 1H); ^{13}C NMR (100 MHz, [D$_6$]DMSO): δ= 106.1, 112.8, 113.0, 113.6, 121.4, 122.1, 123.6, 124.5, 124.8, 127.1, 127.2, 137.3, 138.2, 139.5, 143.5, 153.8, 163.2, 182.7 ppm; IR (solid): $\tilde{\nu}$=3282, 1669, 1605, 1588, 1573, 1495, 1440, 1412, 1240, 1114, 1007, 829, 783, 712, 687, 659 cm^{-1}; MS (ES): *m/z* (%): 331 (100) [*M*+H]$^+$; HRMS-ES: *m/z* [*M*+H]$^+$ calcd for $C_{20}H_{15}N_2O_3$: 331.1083, found: 331.1067.

2-(1*H*-Indol-3-yl)-2-oxo-*N*-(4-(thiophen-2-yl)phenyl)acetamide (1p): Golden yellow solid (64 mg, 9%): ^{1}H NMR (400 MHz, [D$_6$]DMSO): δ=12.38 (s, 1H), 10.38 (s, 1H), 8.80 (d, J=2.5 Hz, 1H), 8.33–8.28 (m, 1H), 7.94 (d, J=9.0 Hz, 2H), 7.69 (d, J=9.0 Hz, 2H), 7.60–7.55 (m, 1H), 7.54–7.48 (m, 2H), 7.34–7.28 (m, 2H), 7.14 ppm (dd, J=3.5 Hz, 5.0 Hz, 1H); ^{13}C NMR (100 MHz, [D$_6$]DMSO): δ= 111.9, 112.7, 120.7, 121.2, 122.7, 123.2, 123.6, 125.2, 125.8, 126.2, 128.4, 129.7, 136.4, 137.5, 138.6, 143.1, 162.3, 181.7 ppm; IR (solid): $\tilde{\nu}$=3278, 1669, 1606, 1575, 1506, 1441, 1408, 1238, 1123, 814, 781, 716, 688, 661, 598 cm^{-1}; MS (ES): *m/z* (%): 347 (100) [*M*+H]$^+$; HRMS-ES: *m/z* [*M*+H]$^+$ calcd for $C_{20}H_{15}N_2O_2S$: 347.0854, found: 347.0862.

***N*-(4-(1*H*-Pyrazol-1-yl)phenyl)-2-(1-methyl-1*H*-indol-3-yl)-2-oxoacetamide (7a)**: Crystalline, pale orange solid (151 mg, 29%): ^{1}H NMR (400 MHz, [D$_6$]DMSO): δ=10.87 (s, 1H), 8.86 (s, 1H), 8.49 (d, J=2.5 Hz, 1H), 8.35–8.30 (m, 1H), 8.02 (d, J=9.0 Hz, 2H), 7.87 (d, J=9.0 Hz, 2H), 7.75 (d, J=1.5 Hz, 1H), 7.66–7.62 (m, 1H), 7.41–7.33 (m, 2H), 6.55 (dd, J=2.0 Hz, 2.5 Hz), 3.95 ppm (s, 3H); ^{13}C NMR (100 MHz, [D$_6$]DMSO): δ=33.4, 107.7, 110.8, 111.2, 118.7, 121.0, 121.3, 123.1, 123.6, 126.7, 127.5, 135.9, 136.2, 137.1, 140.7, 142.0, 162.2, 181.2 ppm; IR (solid): $\tilde{\nu}$=3343, 3096, 1683, 1622, 1524, 1502, 1463, 1369, 1123, 1083, 838, 788, 748, 652 cm^{-1}; MS (ES): *m/z* (%): 345 (100) [*M*+H]$^+$; HRMS-ES: *m/z* [*M*+H]$^+$ calcd for $C_{20}H_{17}N_4O_2$: 345.1352, found: 345.1358.

***N*-(4-(1*H*-Pyrazol-1-yl)phenyl)-2-(1-ethyl-1*H*-indol-3-yl)-2-oxoacetamide (7b)**: Yellow to orange powder (126 mg, 23%): ^{1}H NMR (400 MHz, [D$_6$]DMSO): δ=10.88 (s, 1H), 8.89 (s, 1H), 8.49 (d, J=2.5 Hz, 1H), 8.36–8.31 (m, 1H), 8.02 (d, J=9.0 Hz, 2H), 7.87 (d, J=9.0 Hz, 2H), 7.75 (d, J=1.5 Hz, 1H), 7.72–7.67 (m, 1H), 7.40–7.33 (m, 2H), 6.55 (t, J=2.0 Hz, 1H), 4.39 (q, J=7.0 Hz, 2H), 1.44 ppm (t, J=7.0 Hz, 3H); ^{13}C NMR (100 MHz, [D$_6$]DMSO): δ=16.0, 42.4, 108.6, 111.9, 112.1, 119.6, 121.9, 122.4, 124.0, 124.5, 127.8, 128.4, 136.8, 137.0, 137.1, 141.5, 141.6, 163.1, 182.1 ppm; IR (solid): $\tilde{\nu}$=3350, 3127, 1682, 1617, 1593, 1532, 1502, 1484, 1388, 1311, 1220, 1169, 1129, 1050, 934, 872, 823, 788 cm^{-1}; MS (ES): *m/z* (%): 359 (100) [*M*+H]$^+$; HRMS-ES: *m/z* [*M*+H]$^+$ calcd for $C_{21}H_{19}N_4O_2$: 359.1508, found: 359.1518.

***N*-(4-(1*H*-Pyrazol-1-yl)phenyl)-2-(1-isopropyl-1*H*-indol-3-yl)-2-oxoacetamide (7c)**: Pale orange powder (124 mg, 22%): ^{1}H NMR (400 MHz, [D$_6$]DMSO): δ=10.88 (s, 1H), 8.88 (s, 1H), 8.49 (d, J=2.0 Hz, 1H), 8.37–8.33 (m, 1H), 8.02 (d, J=8.5 Hz, 2H), 7.87 (d, J=8.5 Hz, 2H), 7.78–7.72 (m, 2H), 7.39–7.33 (m, 2H), 6.55 (t, J=2.0 Hz, 1H), 4.91 (septet, J=6.5 Hz, 1H), 1.56 ppm (d, J=6.5 Hz, 6H); ^{13}C NMR (100 MHz, [D$_6$]DMSO): δ=22.9, 49.0, 108.6, 112.1, 112.4, 119.6, 122.0, 122.4, 124.1, 124.5, 127.8, 128.4, 136.8, 137.0, 138.2, 141.6, 163.1, 182.0 ppm; IR (solid): $\tilde{\nu}$=3351, 3129, 2976, 1685, 1625, 1596, 1532, 1497, 1412, 1402, 1382, 1305, 1218, 1170, 827, 787, 755, 734, 665, 650 cm^{-1}; MS (ES): *m/z* (%): 373 (100) [*M*+H]$^+$; HRMS-ES: *m/z* [*M*+H]$^+$ calcd for $C_{22}H_{21}N_4O_2$: 373.1665, found: 373.1676.

***N*-(4-(1*H*-Pyrazol-1-yl)phenyl)-2-(1-(cyclopropylmethyl)-1*H*-indol-3-yl)-2-oxoacetamide (7d)**: Microcrystalline, bright yellow solid (337 mg, 59%): ^{1}H NMR (400 MHz, [D$_6$]DMSO): δ=10.89 (s, 1H), 8.94 (s, 1H), 8.49 (d, J=2.5 Hz, 1H), 8.36–8.32 (m, 1H), 8.02 (d, J=9.0 Hz, 2H), 7.87 (d, J=9.0 Hz, 2H), 7.77–7.71 (m, 2H), 7.39–7.33 (m, 2H), 6.55 (dd, J=1.8 Hz, 2.2 Hz, 1H), 4.23 (d, J=7.5 Hz, 2H), 1.41–1.30 (m, 1H), 0.59–0.54 (m, 2H), 0.49–0.43 ppm (m, 2H); ^{13}C NMR (100 MHz, [D$_6$]DMSO): δ=3.8, 11.1, 50.5, 107.7, 111.0, 111.4, 118.7, 121.0, 121.4, 123.1, 123.6, 126.8, 127.5, 135.9, 136.2, 136.5, 140.70, 140.74, 162.2, 181.2 ppm; IR (solid): $\tilde{\nu}$=3342, 3126, 3001, 1678, 1616, 1595, 1522, 1502, 1486, 1393, 1376, 1220, 1175, 1050, 934, 829, 745, 674, 655, 613 cm^{-1}; MS (ES): *m/z* (%): 385 (100) [*M*+H]$^+$; HRMS-ES: *m/z* [*M*+H]$^+$ calcd for $C_{23}H_{21}N_4O_2$: 385.1665, found: 385.1656.

***N*-(4-(1*H*-Pyrazol-1-yl)phenyl)-2-(1-cyclopropyl-1*H*-indol-3-yl)-2-oxoacetamide (7e)**: Bright yellow powder (83 mg, 15%): ^{1}H NMR (400 MHz, [D$_6$]DMSO): δ=10.87 (s, 1H), 8.72 (s, 1H), 8.49 (d, J=2.5 Hz, 1H), 8.34–8.29 (m, 1H), 8.01 (d, J=9.0 Hz, 2H), 7.86 (d, J=9.0 Hz, 2H), 7.77–7.72 (m, 2H), 7.43–7.35 (m, 2H), 6.55 (t, J=2.0 Hz, 1H), 3.71–3.63 (m, 1H), 1.20–1.12 (m, 2H), 1.11–1.06 ppm (m, 2H); ^{13}C NMR (100 MHz, [D$_6$]DMSO): δ=5.9, 28.1, 107.7, 111.0, 111.6, 118.7, 121.1, 121.5, 123.5, 123.9, 126.8, 127.5, 136.0, 136.1, 137.6, 140.4, 140.7, 162.0, 181.3 ppm; IR (solid): $\tilde{\nu}$=3342, 3154, 3010, 1684, 1622, 1534, 1495, 1482, 1465, 1359, 1313, 1224, 1168, 1024, 934, 870, 831, 785, 759, 738, 726, 674, 651, 609 cm^{-1}; MS (ES): *m/z* (%): 371 (100) [*M*+H]$^+$; HRMS-ES: *m/z* [*M*+H]$^+$ calcd for $C_{22}H_{19}N_4O_2$: 371.1508, found: 371.1508.

2-Chloro-1-(1*H*-indol-3-yl)ethanone (8): Pyridine (8.1 mL, 0.1 mol) was added to a suspension of indole (11.7 g, 0.1 mol) in dry dioxane (100 mL) under N_2. The resultant mixture was warmed to 60 °C then chloroacetyl chloride (8.0 mL, 11.3 g, 0.1 mol) was added dropwise over 10 min. The reaction mixture was maintained at 60 °C for 1 h then poured over water (200 mL) and extracted into EtOAc. The organic layer was washed with brine, dried ($MgSO_4$), filtered and concentrated in vacuo. The oily residue was crystallised from MeOH, then the solids triturated with MeCN to afford the title compound as a pale brown powder (2.4 g, 13%): ^{1}H NMR (400 MHz, [D$_6$]DMSO): δ=12.16 (s, 1H), 8.46 (d, J=2.9 Hz, 1H), 8.18 (d, J=7.1 Hz, 1H), 7.51 (d, J=7.7 Hz, 1H), 7.29–7.20 (m, 2H), 4.90 ppm (s, 2H); ^{13}C NMR (100 MHz, [D$_6$]DMSO): δ=46.4, 112.3, 113.6, 121.1, 122.1, 123.2, 125.4, 134.7, 136.6, 186.1 ppm; IR (solid): $\tilde{\nu}$=3179, 2944, 1639, 1579, 1516, 1490, 1457, 1427, 1398, 1338, 1315, 1278, 1236, 1152, 1138, 1096, 1007, 952, 919, 792, 759 cm^{-1}; MS (ES): *m/z* (%): 193 (100) [*M*]$^+$; HRMS-ES: *m/z* [*M*]$^+$ calcd for $C_{10}H_9ClNO$: 193.0294, found: 193.0292.

General synthesis of indole-3-(2-aminoacetyl) derivatives (2a–d): *N*,*N*-Diisopropylethylamine (DIPEA; 0.45 mL, 0.33 g, 2.6 mmol) and KI (45 mg, 0.3 mmol) were added to a suspension of **8** (388 mg, 2.0 mmol) in dry MeCN (8 mL) under N_2. The respective amine (2.2 mmol) was added, and the mixture heated at reflux for 18 h. After thorough mixing with water (8 mL) and concentration in vacuo, the resultant solids were washed with water then triturated in hot MeCN to afford the product.

2-Anilino-1-(1*H*-indol-3-yl)ethanone (2a): Cream coloured solid (33 mg, 7%): ^{1}H NMR (400 MHz, [D$_6$]DMSO): δ=12.07 (s, 1H), 8.58 (d, J=3.0 Hz, 1H), 8.21 (d, J=6.8 Hz, 1H), 7.51 (dd, J=1.6 Hz, 6.7 Hz, 1H), 7.23 (dq, J=3.6 Hz, 7.1 Hz, 2H), 7.09 (t, J=7.8 Hz, 2H), 6.70 (d, J=7.8 Hz, 2H), 6.56 (t, J=7.2 Hz, 1H), 5.89 (t, J=5.4 Hz, 1H), 4.48 ppm (d, J=5.5 Hz, 2H); ^{13}C NMR (100 MHz, [D$_6$]DMSO): δ=49.8, 112.2, 112.4, 114.2, 115.9, 121.2, 121.8, 122.8, 125.4, 128.8, 133.7, 136.4, 148.4, 191.8 ppm; IR (solid): $\tilde{\nu}$=3326, 1644, 1602, 1528, 1496, 1429, 1413, 1340, 1311, 1246, 1179, 1158, 1106, 1094, 1010, 986, 947, 883 cm^{-1}; MS (ES): *m/z* (%): 251 (100) [*M*+H]$^+$;

HRMS-ES: *m/z* $[M+H]^+$ calcd for $C_{16}H_{15}N_2O$: 251.1184, found: 251.1177.

1-(1*H*-Indol-3-yl)-2-((4-methoxyphenyl)amino)ethanone (2b): Brown solid (50 mg, 9%): ^{1}H NMR (400 MHz, [D$_6$]DMSO): δ = 12.07 (s, 1H), 8.57 (s, 1H), 8.20 (dd, *J* = 1.9 Hz, 6.6 Hz, 1H), 7.50 (dd, *J* = 1.6 Hz, 6.7 Hz, 1H), 7.22 (dq, *J* = 3.6 Hz, 7.1 Hz, 2H), 6.73 (d, *J* = 8.9 Hz, 2H), 6.66 (d, *J* = 9.0 Hz, 2H), 5.50 (t, *J* = 5.6 Hz, 1H), 4.42 (d, *J* = 5.6 Hz, 2H), 3.64 ppm (s, 3H); ^{13}C NMR (100 MHz, [D$_6$]DMSO): δ = 50.6, 55.3, 112.1, 113.4, 114.3, 114.5, 121.2, 121.8, 122.8, 123.6, 125.4, 133.6, 136.4, 142.7, 150.9, 192.2 ppm; MS (ES): *m/z* (%): 281 (100) $[M+H]^+$; HRMS-ES: *m/z* $[M+H]^+$ calcd for $C_{17}H_{17}N_2O_2$: 281.1290, found: 281.1278.

1-(1*H*-Indol-3-yl)-2-((4-morpholinophenyl)amino)ethanone (2c): Yellow solid (250 mg, 37%): ^{1}H NMR (400 MHz, [D$_6$]DMSO): δ = 12.17 (s, 1H), 8.57 (s, 1H), 8.20 (d, *J* = 6.9 Hz, 1H), 7.50 (d, *J* = 7.2 Hz, 1H), 7.21 (t, *J* = 6.2 Hz, 2H), 6.76 (d, *J* = 8.7 Hz, 2H), 6.64 (d, *J* = 8.7 Hz, 2H), 5.49 (t, *J* = 5.4 Hz, 1H), 4.42 (d, *J* = 5.5 Hz, 2H), 3.71 (t, *J* = 4.2 Hz, 4H), 2.90 ppm (t, *J* = 4.3 Hz, 4H); ^{13}C NMR (100 MHz, [D$_6$]DMSO): δ = 50.5, 66.3, 112.2, 113.2, 114.3, 117.5, 121.2, 121.8, 122.8, 125.4, 133.7, 136.4, 142.6, 192.3 ppm; MS (ES): *m/z* (%): 336 (100) $[M+H]^+$; HRMS-ES: *m/z* $[M+H]^+$ calcd for $C_{20}H_{22}N_3O_2$: 336.1712, found: 336.1707.

2-(Benzylamino)-1-(1*H*-indol-3-yl)ethanone (2d): Cream coloured solid (39 mg, 7%): ^{1}H NMR (400 MHz, [D$_6$]DMSO): δ = 12.57 (s, 1H), 9.75 (s, 1H), 8.48 (d, *J* = 2.4 Hz, 1H), 8.17 (d, *J* = 6.6 Hz, 1H), 7.63 (d, *J* = 7.3 Hz, 1H), 7.55 (d, *J* = 7.9 Hz, 1H), 7.47–7.41 (m, 3H), 7.29–7.23 (m, 2H), 4.54 (s, 2H), 4.22 ppm (s, 2H); ^{13}C NMR (100 MHz, [D$_6$]DMSO): δ = 50.1, 50.8, 112.5, 113.2, 120.9, 122.3, 123.3, 125.0, 128.6, 128.9, 130.2, 131.9, 135.2, 136.6, 185.7 ppm; IR (solid): $\tilde{\nu}$ = 3335, 3085, 3015, 2903, 2854, 2766, 2612, 1801, 1626, 1613, 1520, 1411, 1246, 1149, 1060, 1040, 1000, 949, 904, 857, 784 cm^{-1}; MS (ES): *m/z* (%): 265 (100) $[M+H]^+$; HRMS-ES: *m/z* $[M+H]^+$ calcd for $C_{17}H_{17}N_2O$: 265.1341, found: 265.1332.

General synthesis of indole-3-acetamide compounds (3a–d): DIPEA (0.77 mL, 0.57 g, 4.4 mmol), indole-3-acetic acid (350 mg, 2.0 mmol) and benzotriazol-1-yloxytripyrrolidinophosphonium hexafluorophosphate (1.04 g, 2.0 mmol) were combined in $CHCl_3$ (7 mL), then the requisite primary amine (2.2 mmol) was added and the mixture stirred at RT for 18 h. Where the product had precipitated from the reaction mixture (**3b**, **3c**), it was collected by filtration and washed with $CHCl_3$. Otherwise (**3a**, **3d**), the reaction mixture was stirred vigorously with 1 M HCl (10 mL), then the upper layer removed by suction. The organic phase was washed with brine, dried ($MgSO_4$), filtered and concentrated. The crude material was purified by flash column chromatography on silica (1:1, EtOAc/hexane).

2-(1*H*-Indol-3-yl)-*N*-phenylacetamide (3a): Cream coloured solid (366 mg, 73%): ^{1}H NMR (400 MHz, [D$_6$]DMSO): δ = 10.94 (s, 1H), 10.12 (s, 1H), 7.64–7.60 (m, 3H), 7.37 (d, *J* = 8.1 Hz, 1H), 7.32–7.26 (m, 3H), 7.08 (t, *J* = 7.5 Hz, 1H), 7.05–6.97 (m, 2H), 3.75 ppm (s, 2H); ^{13}C NMR (100 MHz, [D$_6$]DMSO): δ = 33.8, 108.6, 111.3, 118.4, 118.7, 119.1, 121.0, 123.0, 123.8, 127.2, 128.6, 136.1, 139.4, 169.7 ppm; IR (solid): $\tilde{\nu}$ = 3421, 3238, 3189, 3127, 3060, 1652, 1618, 1596, 1540, 1487, 1457, 1442, 1339, 1270, 1222, 1165, 1092, 1051, 1008, 974, 901, 849, 784, 758 cm^{-1}; MS (ES): *m/z* (%): 251 (100) $[M+H]^+$; HRMS-ES: *m/z* $[M+H]^+$ calcd for $C_{16}H_{15}N_2O$: 251.1184, found: 251.1187.

2-(1*H*-Indol-3-yl)-*N*-(4-methoxyphenyl)acetamide (3b): White solid (330 mg, 59%): ^{1}H NMR (400 MHz, [D$_6$]DMSO): δ = 10.92 (s, 1H), 9.97 (s, 1H), 7.62 (d, *J* = 7.9 Hz, 1H), 7.52 (d, *J* = 7.9 Hz, 2H), 7.36 (d, *J* = 7.9 Hz, 1H), 7.26 (d, *J* = 7.9 Hz, 1H), 7.08 (t, *J* = 7.1 Hz, 1H), 6.99 (t, *J* = 7.4 Hz, 1H), 6.87 (d, *J* = 7.9 Hz, 2H), 3.71 ppm (s, 5H); ^{13}C NMR (100 MHz, [D$_6$]DMSO): δ = 33.7, 55.1, 108.7, 111.3, 113.8, 118.3, 118.7, 120.6, 120.9, 123.8, 127.2, 132.6, 136.1, 155.0, 169.2 ppm; IR (solid): $\tilde{\nu}$ = 3411, 3236, 3121, 3060, 3007, 1649, 1604, 1604, 1544, 1506, 1456, 1438, 1408, 1354, 1299, 1271, 1246, 1222, 1164, 1095, 1031, 979, 829, 779 cm^{-1}; MS (ES): *m/z* (%): 281 (100) $[M+H]^+$; HRMS-ES: *m/z* $[M+H]^+$ calcd for $C_{17}H_{17}N_2O_2$: 281.1290, found: 281.1288.

2-(1*H*-Indol-3-yl)-*N*-(4-morpholinophenyl)acetamide (3c): White solid (479 mg, 71%): ^{1}H NMR (400 MHz, [D$_6$]DMSO): δ = 10.92 (s, 1H), 9.91 (s, 1H), 7.62 (d, *J* = 7.9 Hz, 1H), 7.48 (d, *J* = 9.0 Hz, 2H), 7.36 (d, *J* = 8.1 Hz, 1H), 7.25 (d, *J* = 2.2 Hz, 1H), 7.08 (t, *J* = 7.5 Hz, 1H), 6.99 (t, *J* = 7.4 Hz, 1H), 6.88 (d, *J* = 9.1 Hz, 2H), 3.72 (t, *J* = 7.9 Hz, 4H), 3.69 (s, 2H), 3.02 ppm (t, *J* = 7.9 Hz, 4H); ^{13}C NMR (100 MHz, [D$_6$]DMSO): δ = 33.7, 49.0, 66.1, 108.8, 111.3, 115.4, 118.3, 118.7, 120.2, 120.9, 123.8, 127.2, 131.7, 136.1, 147.1, 169.1 ppm; IR (solid): $\tilde{\nu}$ = 3402, 1646, 1600, 1541, 1512, 1457, 1446, 1416, 1330, 1249, 1221, 1166, 1118, 1098, 1052, 1009, 980, 931, 855, 813 cm^{-1}; MS (ES): *m/z* (%): 336 (100) $[M+H]^+$; HRMS-ES: *m/z* $[M+H]^+$ calcd for $C_{20}H_{22}N_3O_2$: 336.1712, found: 336.1714.

***N*-Benzyl-2-(1*H*-indol-3-yl)acetamide (3d)**: White solid (190 mg, 36%): ^{1}H NMR (400 MHz, [D$_6$]DMSO): δ = 10.90 (s, 1H), 8.42 (t, *J* = 5.9 Hz, 1H), 7.57 (d, *J* = 7.8 Hz, 1H), 7.36 (d, *J* = 8.1 Hz, 1H), 7.29 (dd, *J* = 6.6 Hz, 7.8 Hz, 2H), 7.22 (dd, *J* = 4.8 Hz, 8.6 Hz, 4H), 7.08 (t, *J* = 7.0 Hz, 1H), 6.98 (t, *J* = 7.4 Hz, 1H), 4.28 (d, *J* = 6.0 Hz, 2H), 3.59 ppm (s, 2H); ^{13}C NMR (100 MHz, [D$_6$]DMSO): δ = 32.7, 42.2, 108.8, 111.3, 118.2, 118.7, 120.9, 123.8, 126.7, 127.2, 128.2, 136.1, 139.6, 170.7 ppm; IR (solid): $\tilde{\nu}$ = 3269, 3084, 1627, 1616, 1558, 1494, 1452, 1423, 1356, 1340, 1279, 1245, 1225, 1172, 1128, 1102, 1043, 1022, 946, 879, 798 cm^{-1}; MS (ES): *m/z* (%): 265 (100) $[M+H]^+$; HRMS-ES: *m/z* $[M+H]^+$ calcd for $C_{17}H_{17}N_2O$: 265.1341, found: 265.1345.

3-Hydroxy-4-(1*H*-indol-3-yl)-1*H*-pyrrole-2,5-dione (9): Indol-3-ylacetamide (4.8 g, 30 mmol) was suspended in dry DMF (100 mL) under N_2, then dimethyl oxalate (3.9 g, 33 mmol) was added, and the reaction mixture cooled to 0 °C. Potassium *tert*-butoxide (7.4 g, 66 mmol) was added portionwise over 10 min. After 30 min, the cooling was removed and the reaction mixture stirred at RT for 18 h, then poured into water (400 mL). The solution was acidified by careful addition of 6 M HCl, then extracted into EtOAc. The organic layer was separated, washed with brine, then dried ($MgSO_4$), filtered and concentrated to provide the title compound as a red solid (6.2 g, 96%): ^{1}H NMR (400 MHz, [D$_6$]DMSO): δ = 11.72 (s, 1H), 11.52 (s, 1H), 10.54 (s, 1H), 8.11 (d, *J* = 8.0 Hz, 1H), 7.84 (d, *J* = 2.7 Hz, 1H), 7.41 (d, *J* = 8.1 Hz, 1H), 7.14 (t, *J* = 7.1 Hz, 1H), 7.04 ppm (t, *J* = 7.5 Hz, 1H); ^{13}C NMR (100 MHz, [D$_6$]DMSO): δ = 104.3, 106.6, 111.5, 119.2, 121.6, 122.1, 125.5, 126.3, 136.0, 147.3, 168.8, 172.6 ppm; IR (solid): $\tilde{\nu}$ = 3420, 3242, 2691, 1942, 1772, 1680, 1616, 1522, 1490, 1460, 1426, 1388, 1353, 1290, 1254, 1238, 1187, 1142, 1104, 1074, 1011, 974, 869, 840 cm^{-1}; MS (ES): *m/z* (%): 228 (100) $[M]^+$; HRMS-ES: *m/z* $[M]^+$ calcd for $C_{12}H_8N_2O_3$: 228.0535, found: 228.0539.

General synthesis of maleimide-bridged compounds (4a–d): The appropriate amine (1.1 mmol) was added to a suspension of **9** (228 mg, 1.0 mmol) in AcOH/H_2O (1:1, 6 mL). The mixture was heated at reflux for 3 h, concentrated in vacuo, and the residue partitioned between saturated aq $NaHCO_3$ and EtOAc. The organic phase was washed with brine, dried ($MgSO_4$), filtered and concentrated. The crude material was purified by flash column chromatography on silica (1:1, EtOAc/hexane).

3-Anilino-4-(1*H*-indol-3-yl)pyrrole-2,5-dione (4a): Red solid (197 mg, 65%): ^{1}H NMR (400 MHz, [D$_6$]DMSO): δ = 11.23 (s, 1H), 10.67 (s, 1H), 9.14 (s, 1H), 7.36 (d, J = 7.9 Hz, 1H), 7.27 (d, J = 8.1 Hz, 1H), 6.99–6.96 (m, 2H), 6.87–6.79 (m, 3H), 6.75–6.67 ppm (m, 3H); ^{13}C NMR (100 MHz, [D$_6$]DMSO): δ = 102.8, 104.8, 111.1, 118.8, 119.6, 120.5, 121.0, 121.8, 126.7, 127.4, 134.8, 135.3, 138.6, 169.9, 173.0 ppm; IR (solid): $\tilde{\nu}$ = 3277, 3046, 2924, 2836, 1759, 1696, 1646, 1615, 1507, 1456, 1417, 1354, 1300, 1238, 1173, 1131, 1100, 1026, 1010, 901, 825 cm^{-1}; MS (ES): *m/z* (%): 304 (100) $[M+H]^+$; HRMS-ES: *m/z* $[M+H]^+$ calcd for $C_{18}H_{14}N_3O_2$: 304.1086, found: 304.1087.

3-(1*H*-Indol-3-yl)-4-((4-methoxyphenyl)amino)pyrrole-2,5-dione (4b): Red solid (233 mg, 70%): ^{1}H NMR (400 MHz, [D$_6$]DMSO): δ = 11.13 (s, 1H), 10.58 (s, 1H), 9.03 (s, 1H), 7.38 (d, J = 8.0 Hz, 1H), 7.27 (d, J = 8.1 Hz, 1H), 6.99 (t, J = 7.1 Hz, 1H), 6.84 (t, J = 7.1 Hz, 1H), 6.76 (d, J = 2.4 Hz, 1H), 6.66 (d, J = 8.9 Hz, 2H), 6.42 (d, J = 9.0 Hz, 2H), 3.54 ppm (s, 3H); ^{13}C NMR (100 MHz, [D$_6$]DMSO): δ = 55.0, 99.3, 104.7, 111.0, 112.6, 118.7, 120.6, 120.9, 121.8, 126.5, 126.8, 131.2, 135.3, 136.0, 154.8, 169.8, 173.1 ppm; IR (solid): $\tilde{\nu}$ = 3278, 3046, 2930, 2837, 1757, 1696, 1645, 1615, 1506, 1457, 1418, 1353, 1300, 1237, 1173, 1129, 1105, 1028, 1011, 902, 824, 764 cm^{-1}; MS (ES): *m/z* (%): 334 (100) $[M+H]^+$; HRMS-ES: *m/z* $[M+H]^+$ calcd for $C_{19}H_{16}N_3O_3$: 334.1192, found: 334.1178.

3-(1*H*-Indol-3-yl)-4-((4-morpholinophenyl)amino)pyrrole-2,5-dione (4c): Red solid (34 mg, 4%): ^{1}H NMR (400 MHz, [D$_6$]DMSO): δ = 11.17 (s, 1H), 10.57 (s, 1H), 9.00 (s, 1H), 7.38 (d, J = 8.0 Hz, 1H), 7.27 (d, J = 8.1 Hz, 1H), 6.99 (t, J = 7.5 Hz, 1H), 6.83 (t, J = 7.5 Hz, 1H), 6.71 (d, J = 2.6 Hz, 1H), 6.61 (d, J = 9.0 Hz, 2H), 6.44 (d, J = 9.0 Hz, 2H), 3.63 (t, J = 4.7 Hz, 4H), 2.86 ppm (t, J = 4.7 Hz, 4H); ^{13}C NMR (100 MHz, [D$_6$]DMSO): δ = 48.8, 65.9, 66.3, 99.1, 104.7, 111.0, 114.1, 118.6, 120.6, 120.8, 121.4, 126.5, 130.2, 135.3, 135.8, 146.7, 169.8, 173.1 ppm; IR (solid): $\tilde{\nu}$ = 3423, 3267, 3112, 3046, 2952, 2853, 2757, 1763, 1694, 1644, 1614, 1540, 1512, 1450, 1414, 1344, 1234, 1112, 1068, 1034, 926, 902, 860, 822 cm^{-1}; MS (ES): *m/z* (%): 389 (100) $[M+H]^+$; HRMS-ES: *m/z* $[M+H]^+$ calcd for $C_{22}H_{21}N_4O_3$: 389.1614, found: 389.1618.

3-(Benzylamino)-4-(1*H*-indol-3-yl)pyrrole-2,5-dione (4d): Yellow solid (33 mg, 5%): ^{1}H NMR (400 MHz, [D$_6$]DMSO): δ = 11.23 (s, 1H), 10.39 (s, 1H), 7.55 (t, J = 6.8 Hz, 1H), 7.39 (d, J = 8.1 Hz, 1H), 7.32 (d, J = 7.9 Hz, 1H), 7.15–7.08 (m, 5H), 6.98 (t, J = 7.4 Hz, 1H), 6.86–6.83 (m, 2H), 4.22 ppm (d, J = 6.8 Hz, 2H); ^{13}C NMR (100 MHz, [D$_6$]DMSO): δ = 45.6, 93.7, 103.9, 111.4, 118.9, 119.5, 121.1, 125.9, 126.7, 126.9, 128.0, 128.4, 135.5, 139.1, 143.1, 169.1, 173.2 ppm; IR (solid): $\tilde{\nu}$ = 3409, 3170, 3058, 1764, 1703, 1646, 1616, 1553, 1504, 1454, 1429, 1415, 1357, 1239, 1098, 1070, 1020, 908, 870, 826, 754 cm^{-1}; MS (ES): *m/z* (%): 318 (100) $[M+H]^+$; HRMS-ES: *m/z* $[M+H]^+$ calcd for $C_{19}H_{16}N_3O_2$: 318.1234, found: 318.1253.

Ethyl 3-(1*H*-indol-3-yl)-3-oxopropanoate (10): Indole (1.70 g, 15 mmol) was added to a solution of mono-ethyl malonate (3.96 g, 30 mmol) in Ac_2O (40 mL). The mixture was stirred at 85 °C for 3 h, then allowed to cool to RT, and poured carefully into ice-cold water (100 mL). After stirring vigorously for 1 h, the mixture was evaporated to dryness, and the residue triturated thoroughly with saturated aq $NaHCO_3$ (15 mL), then extracted into EtOAc. The aqueous layer was extracted once with EtOAc, and the combined organic extracts were dried ($MgSO_4$), filtered and concentrated. The resultant dark red oil was purified by column chromatography on silica (50→60→70→80→90→100%, CH_2Cl_2/hexane) to provide the title compound as a viscous, pale yellow oil (1.33 g, 38%): R_f = 0.30 (CH_2Cl_2/hexane, 7:3); ^{1}H NMR (400 MHz, $CDCl_3$): δ = 8.48 (d, J = 8.0 Hz, 1H), 7.59 (d, J = 7.5 Hz, 1H), 7.42–7.37 (m, 2H), 7.32 (dt, J = 1.0 Hz, 7.5 Hz, 1H), 6.71–6.68 (m, 1H), 4.28 (q, J = 7.0 Hz, 2H), 3.98 (s, 2H), 1.31 ppm (t, J = 7.0 Hz, 3H); ^{13}C NMR (100 MHz, $CDCl_3$): δ = 14.1, 43.9, 62.1, 110.2, 116.7, 121.0, 124.2, 124.7, 125.5, 130.5, 135.7, 164.0, 166.2 ppm; IR (neat): $\tilde{\nu}$ = 3140, 3049, 2980, 2953, 2904, 1742, 1706, 1534, 1451, 1381, 1360, 1313, 1267, 1205, 1174, 1151, 1108, 1038, 925, 769 cm^{-1}; MS (ES): *m/z* (%): 232 (100) $[M+H]^+$; HRMS-ES: *m/z* $[M+H]^+$ calcd for $C_{13}H_{14}NO_3$: 232.0974, found: 232.0971.

Benzyl 3-(1*H*-indol-3-yl)-3-oxopropanoate (11): Indole (1.21 g, 10.5 mmol) and mono-benzyl malonate (4.0 g, 21 mmol) were combined in Ac_2O (40 mL), and the solution heated at 85 °C for 3 h, then allowed to cool to RT. Work-up and column chromatography as for **10** afforded benzyl ester **11** as a white solid (1.65 g, 54%): ^{1}H NMR (400 MHz, $CDCl_3$): δ = 8.48 (d, J = 7.5 Hz, 1H), 7.59 (d, J = 7.5 Hz, 1H), 7.43–7.30 (m, 8H), 6.67 (d, J = 3.5 Hz, 1H), 5.26 (s, 2H), 4.04 ppm (s, 2H); ^{13}C NMR (100 MHz, $CDCl_3$): δ = 43.8, 67.7, 110.3, 116.7, 121.0, 124.2, 124.6, 125.5, 128.4, 128.5, 128.6, 130.4, 135.0, 163.8, 166.0 ppm; IR (solid): $\tilde{\nu}$ = 3138, 3065, 3029, 2950, 2896, 1741, 1707, 1533, 1450, 1414, 1380, 1352, 1313, 1265, 1204, 1150, 1107, 999, 924 cm^{-1}; MS (ES): *m/z* (%): 294 (100) $[M+H]^+$; HRMS-ES: *m/z* $[M+H]^+$ calcd for $C_{18}H_{16}NO_3$: 294.1130, found: 294.1121.

Ethyl 4-(1*H*-indol-3-yl)-4-oxobutanoate (13): Diethylaluminium chloride (1.0 M solution in hexane, 19.2 mL, 19.2 mmol) was added to a solution of indole (1.50 g, 12.8 mmol) in dry CH_2Cl_2 (100 mL) under N_2 at 0 °C. After 30 min, a solution of ethyl succinyl chloride (2.73 mL, 3.15 g, 19.2 mmol) was added dropwise to the reaction mixture, which was stirred for a further 2 h then quenched by cautious addition of saturated aq NH_4Cl. The organic phase was separated, and the aqueous layer extracted with additional CH_2Cl_2. The combined organic extracts were washed with saturated aq $NaHCO_3$, separated and concentrated. The residue was purified by column chromatography on silica (20→30→40→50→60, EtOAc/hexane) yielding **13** as a pale yellow oil (1.32 g, 42%): R_f = 0.60 (EtOAc/hexane, 2:1); ^{1}H NMR (400 MHz, [D$_6$]DMSO): δ = 11.96 (s, 1H), 8.38 (d, J = 2.5 Hz, 1H), 8.18–8.14 (m, 1H), 7.49–7.45 (m, 1H), 7.24–7.15 (m, 2H), 4.06 (q, J = 7.0 Hz, 2H), 3.18 (t, J = 6.5 Hz, 2H), 2.64 (t, J = 6.5 Hz, 2H), 1.19 ppm (t, J = 7.0 Hz, 3H); ^{13}C NMR (100 MHz, [D$_6$]DMSO): δ = 13.1, 27.0, 32.4, 58.8, 111.1, 114.8, 120.2, 120.6, 121.7, 124.3, 132.8, 135.5, 171.6, 192.1 ppm; IR (neat): $\tilde{\nu}$ = 3158, 3104, 2984, 2934, 1739, 1614, 1521, 1493, 1442, 1429, 1416, 1371, 1316, 1238, 1179, 1148, 1135, 1100, 1030, 1010, 940, 865, 800, 782, 770 cm^{-1}; MS (ES): *m/z* (%): 246 (100) $[M+H]^+$; HRMS-ES: *m/z* $[M+H]^+$ calcd for $C_{14}H_{16}NO_3$: 246.1130, found: 246.1127.

4-(1*H*-Indol-3-yl)-4-oxobutanoic acid (14): A mixture of **13** (1.0 g, 4.1 mmol) and 2.5% *w/v* aq KOH (40 mL) was stirred for 4 h at RT, then acidified to pH 2 using concd HCl. The resulting suspension was extracted into CH_2Cl_2, then the organic layer separated and concentrated to give acid **14** as a white solid (0.48 g, 54%): ^{1}H NMR (400 MHz, D_2O): δ = 8.10 (s, 1H), 8.05–8.00 (m, 1H), 7.46–7.40 (m, 1H), 7.24–7.16 (m, 2H), 3.02 (t, J = 7.5 Hz, 2H), 2.42 ppm (t, J = 7.0 Hz, 2H); ^{13}C NMR (100 MHz, [D$_6$]DMSO): δ = 28.1, 33.5, 112.1, 116.0, 121.2, 121.6, 122.6, 125.3, 133.7, 136.5, 174.1, 193.4 ppm; IR (solid): $\tilde{\nu}$ = 3271, 3064, 2925, 1692, 1630, 1616, 1527, 1440, 1406, 1252, 1134, 972 cm^{-1}; MS (ES): *m/z* (%): 218 (100) $[M+H]^+$; HRMS-ES: *m/z* $[M+H]^+$ calcd for $C_{12}H_{12}NO_3$: 218.0817, found: 218.0816.

General synthesis of two-carbon bridged analogues (6a–d): DIPEA (383 μL, 284 mg, 2.2 mmol), acid **14** (217 mg, 1.0 mmol) and benzotriazol-1-yloxytripyrrolidinophosphonium hexafluorophosphate (0.52 g, 1.0 mmol) were combined in $CHCl_3$ (4 mL), then the requisite primary amine (1.1 mmol) was added, and the mixture stirred at RT for 18 h. Where the product had precipitated from the reaction mixture (**6c**), it was collected by filtration and washed

with $CHCl_3$. Otherwise, the reaction solution was diluted with $CHCl_3$ and water, then the organic layer separated and concentrated, and the crude product purified as indicated below for each individual example.

4-(1*H*-Indol-3-yl)-4-oxo-*N*-phenylbutanamide (6a): Flash column chromatography on silica (10→20→30→40%, EtOAc/hexane) afforded partially purified material which required additional purification by preparative HPLC (Alltima HP C18 HL 5 μm column; isocratic conditions: 60:40, MeCN/H_2O; flow rate = 20 mL min^{-1}; UV detection at 254 nm). The title compound was obtained as a white solid (93 mg, 32%): ^{1}H NMR (400 MHz, [D$_6$]DMSO): δ = 10.13 (s, 1H), 8.35 (d, J = 8.5 Hz, 1H), 8.00 (d, J = 4.0 Hz, 1H), 7.66–7.59 (m, 3H), 7.35–7.24 (m, 4H), 7.03 (dt, J = 1.0 Hz, 7.5 Hz, 1H), 6.79–6.76 (m, 1H), 3.37 (t, J = 6.5 Hz, 2H), 2.82 ppm (t, J = 6.5 Hz, 2H); ^{13}C NMR (100 MHz, [D$_6$]DMSO): δ = 30.1, 30.4, 108.4, 115.8, 118.9, 120.9, 122.9, 123.4, 124.5, 126.4, 128.7, 130.2, 134.9, 139.3, 170.0, 171.4 ppm; IR (solid): $\tilde{\nu}$ = 3242, 3136, 3051, 2906, 1695, 1651, 1597, 1537, 1498, 1446, 1382, 1362, 1304, 1263, 1199, 1178, 951, 910, 766, 740, 691 cm^{-1}; MS (ES): *m/z* (%): 293 (100) [*M*+H]$^+$; HRMS-ES: *m/z* [*M*+H]$^+$ calcd for $C_{18}H_{17}N_2O_2$: 293.1290, found: 293.1295.

4-(1*H*-Indol-3-yl)-*N*-(4-methoxyphenyl)-4-oxobutanamide (6b): Flash column chromatography on silica (0→1→2→3%, MeOH/CH_2Cl_2) gave a partially purified product with was then triturated thoroughly with CH_2Cl_2/hexane (4:1), filtered, and washed with the same solvent system. The title compound was obtained as an off-white solid (155 mg, 48%): R_f = 0.20 (EtOAc/hexane, 1:2); ^{1}H NMR (400 MHz, [D$_6$]DMSO): δ = 9.99 (s, 1H), 8.35 (d, J = 8.5 Hz, 1H), 7.99 (d, J = 4.0 Hz, 1H), 7.64 (d, J = 8.0 Hz, 1H), 7.53 (d, J = 8.5 Hz, 2H), 7.35–7.24 (m, 2H), 6.88 (d, J = 9.0 Hz, 2H), 6.77 (d, J = 3.5 Hz, 1H), 3.71 (s, 3H), 3.36 (t, J = 6.0 Hz, 2H), 2.78 ppm (t, J = 6.0 Hz, 2H); ^{13}C NMR (100 MHz, [D$_6$]DMSO): δ = 30.2, 30.3, 55.1, 108.3, 113.8, 115.9, 120.4, 120.9, 123.3, 124.5, 126.4, 130.2, 132.5, 134.9, 155.0, 169.4, 171.4 ppm; IR (solid): $\tilde{\nu}$ = 3238, 3132, 3065, 2909, 1699, 1651, 1550, 1511, 1450, 1395, 1309, 1244, 1200, 1176, 1034, 952, 914, 824, 768, 741, 720 cm^{-1}; MS (ES): *m/z* (%): 323 (100) [*M*+H]$^+$; HRMS-ES: *m/z* [*M*+H]$^+$ calcd for $C_{19}H_{19}N_2O_3$: 323.1396, found: 323.1402.

4-(1*H*-Indol-3-yl)-*N*-(4-morpholinophenyl)-4-oxobutanamide (6c): Off-white solid (198 mg, 53%): ^{1}H NMR (400 MHz, [D$_6$]DMSO): δ = 9.92 (s, 1H), 8.35 (d, J = 8.5 Hz, 1H), 8.00 (d, J = 4.0 Hz, 1H), 7.64 (d, J = 7.5 Hz, 1H), 7.48 (d, J = 9.5 Hz, 2H), 7.35–7.23 (m, 2H), 6.89 (d, J = 9.0 Hz, 2H), 6.77 (d, J = 3.5 Hz, 1H), 3.72 (t, J = 4.5 Hz, 4H), 3.35 (t, J = 6.0 Hz, 2H), 3.03 (t, J = 4.5 Hz, 4H), 2.77 ppm (t, J = 5.5 Hz, 2H); ^{13}C NMR (100 MHz, [D$_6$]DMSO): δ = 30.2, 30.3, 48.9, 66.1, 108.3, 115.4, 115.8, 120.0, 120.9, 123.3, 124.5, 126.4, 130.1, 131.7, 134.9, 147.0, 169.2, 171.4 ppm; IR (solid): $\tilde{\nu}$ = 3318, 2963, 2856, 2830, 1699, 1655, 1528, 1451, 1394, 1313, 1120, 916, 820, 744, 728 cm^{-1}; MS (ES): *m/z* (%): 378 (100) [*M*+H]$^+$; HRMS-ES: *m/z* [*M*+H]$^+$ calcd for $C_{22}H_{24}N_3O_3$: 378.1818, found: 378.1823.

4-(1*H*-indol-3-yl)-4-oxo-*N*-*p*-tolylbutanamide (6d): Crude solid was triturated with CH_2Cl_2/hexane (4:1), filtered, and washed with the same solvent system, then a little CH_2Cl_2. Further purification by preparative HPLC, under the same conditions detailed for **6a**, afforded the title compound as a cream coloured solid (83 mg, 27%): ^{1}H NMR (400 MHz, [D$_6$]DMSO): δ = 10.03 (s, 1H), 8.34 (d, J = 8.0 Hz, 1H), 8.00 (d, J = 4.0 Hz, 1H), 7.66–7.61 (m, 1H), 7.49 (d, J = 8.0 Hz, 2H), 7.35–7.24 (m, 2H), 7.10 (d, J = 8.0 Hz, 2H), 6.77 (d, J = 4.0 Hz, 1H), 3.36 (t, J = 7.0 Hz, 2H), 2.79 (t, J = 6.5 Hz, 2H), 2.24 ppm (s, 3H); ^{13}C NMR (100 MHz, [D$_6$]DMSO): δ = 20.4, 30.2, 30.4, 108.3, 115.8, 118.9, 120.9, 123.4, 124.5, 126.4, 129.0, 130.1, 131.8, 134.9, 136.8, 169.7, 171.4 ppm; IR (solid): $\tilde{\nu}$ = 3233, 3178, 3126, 3048, 2908, 1698, 1652, 1601, 1535, 1512, 1450, 1396, 1306, 1292, 1262, 1200, 950, 916, 811, 767, 745, 718 cm^{-1}; MS (ES): *m/z* (%): 307 (100) [*M*+H]$^+$; HRMS-ES: *m/z* [*M*+H]$^+$ calcd for $C_{19}H_{19}N_2O_2$: 307.1447, found: 307.1441.

General synthesis of 1-alkylindoles (15b–d): 1-Methylindole **15a** was sourced commercially. 1-Alkylindoles **15b–d** were prepared according to the following protocol. Indole (3.51 g, 30 mmol), potassium *tert*-butoxide (3.93 g, 35 mmol) and 18-crown-6 (0.80 g, 3.0 mmol) were combined in dry Et_2O (70 mL) under N_2 with vigorous stirring. After 10 min, the alkylating agent (35 mmol) was then added, in four separate portions (i.e. 4×8.75 mmol), over a period of 10 min. The flask was flushed with N_2 then stoppered, and stirring continued for 18 h. Water (50 mL) was added, then the mixture was transferred to a separating funnel and agitated until all solids were dissolved. The aqueous layer was extracted with an additional portion of Et_2O, then the combined organic extracts dried ($MgSO_4$), filtered and concentrated. The crude material was purified by flash column chromatography on silica (5→10→20%, CH_2Cl_2/hexane) affording the pure alkylated product.

1-Ethyl-1*H*-indole (15b): Prepared according to the general procedure above, using EtBr (2.61 mL, 3.81 g, 35 mmol) as an alkylating agent. Obtained as a viscous, colourless oil (3.60 g, 83%): ^{1}H NMR (400 MHz, $CDCl_3$): δ = 7.75–7.71 (m, 1H), 7.45–7.42 (m, 1H), 7.30 (dt, J = 1.0 Hz, 7.0 Hz, 1H), 7.22–7.17 (m, 2H), 6.58 (dd, J = 1.0 Hz, 3.0 Hz, 1H), 4.24 (q, J = 7.0 Hz, 2H), 1.53 ppm (t, J = 7.0 Hz, 3H); ^{13}C NMR (100 MHz, $CDCl_3$): δ = 15.5, 41.0, 101.1, 109.3, 119.3, 121.0, 121.4, 127.1, 128.7, 135.7 ppm; IR (neat): $\tilde{\nu}$ = 3054, 2977, 2934, 1511, 1461, 1312, 1220, 736 cm^{-1}; MS (ES): *m/z* (%): 146 (100) [*M*+H]$^+$; HRMS-ES: *m/z* [*M*+H]$^+$ calcd for $C_{10}H_{12}N$: 146.0970, found: 146.0963.

1-Isopropyl-1*H*-indole (15c): Prepared using 2-iodopropane (3.49 mL, 5.95 g, 35 mmol). Fairly viscous, colourless oil (1.04 g, 22%): ^{1}H NMR (400 MHz, $CDCl_3$): δ = 7.76 (d, J = 7.5 Hz, 1H), 7.50 (d, J = 8.5 Hz, 1H), 7.35–7.30 (m, 2H), 7.23 (dt, J = 1.0 Hz, 7.0 Hz, 1H), 6.64 (d, J = 3.0 Hz, 1H), 4.78 (septet, J = 7.5 Hz, 1H), 1.63 ppm (d, J = 7.0 Hz, 6H); ^{13}C NMR (100 MHz, $CDCl_3$): δ = 22.9, 47.1, 101.2, 109.6, 119.3, 121.1, 121.3, 123.6, 128.7, 135.6 ppm; IR (neat): $\tilde{\nu}$ = 3055, 2974, 2931, 1509, 1460, 1313, 1299, 1222, 1017, 736, 714 cm^{-1}; MS (ES): *m/z* (%): 160 (100) [*M*+H]$^+$; HRMS-ES: *m/z* [*M*+H]$^+$ calcd for $C_{11}H_{14}N$: 160.1126, found: 160.1127.

1-(Cyclopropylmethyl)-1*H*-indole (15d): Prepared using cyclopropylmethyl bromide (3.39 mL, 4.73 g, 35 mmol). Viscous, colourless oil (2.71 g, 53%): ^{1}H NMR (400 MHz, $CDCl_3$): δ = 7.76 (d, J = 7.5 Hz, 1H), 7.48 (d, J = 8.0 Hz, 1H), 7.35–7.30 (m, 2H), 7.25–7.20 (m, 1H), 6.62 (dd, J = 0.5 Hz, 3.0 Hz, 1H), 4.06 (d, J = 7.0 Hz, 2H), 1.42–1.31 (m, 1H), 0.74–0.69 (m, 2H), 0.49–0.43 ppm (m, 2H); ^{13}C NMR (100 MHz, $CDCl_3$): δ = 4.2, 11.4, 50.7, 101.0, 109.5, 119.3, 121.0, 121.4, 127.6, 128.6, 136.2 ppm; IR (neat): $\tilde{\nu}$ = 3056, 3005, 2920, 1510, 1461, 1310, 1218, 1012, 762, 736, 714 cm^{-1}; MS (ES): *m/z* (%): 172 (100) [*M*+H]$^+$; HRMS-ES: *m/z* [*M*+H]$^+$ calcd for $C_{12}H_{14}N$: 172.1126, found: 172.1129.

1-Cyclopropyl-1*H*-indole (15e):[19] Indole (3.40 g, 29 mmol), DMAP (10.65 g, 87 mmol), cyclopropylboronic acid (5.00 g, 58 mmol) and $Cu(OAc)_2$ (0.54 g, 3.0 mmol) were combined in dry toluene (60 mL) under N_2. Sodium bis(trimethylsilyl)amide solution (0.6 M in toluene, 48 mL, 29 mmol) was added, and gentle bubbling of a stream of dry air through the reaction mixture was started. This was continued whilst the temperature was raised to 95 °C, then heating was maintained for 48 h, after which time the dark brown mixture was permitted to cool back to RT, then partitioned between 1 M HCl and EtOAc. The aqueous layer was extracted with an additional

portion of EtOAc, then the combined organic extracts dried (Na_2SO_4), filtered and concentrated giving a thick, brown oil. Purification by flash column chromatography on silica (5→10→20%, CH_2Cl_2/hexane) provided the title compound as a viscous, colourless oil (1.77 g, 39%): ^{1}H NMR (400 MHz, $CDCl_3$): δ = 7.79 (d, J = 8.0 Hz, 1H), 7.74 (dd, J = 1.0 Hz, 8.0 Hz, 1H), 7.41 (dt, J = 1.0 Hz, 7.0 Hz, 1H), 7.31 (dt, J = 1.0 Hz, 7.5 Hz, 1H), 7.28 (d, J = 3.0 Hz, 1H), 6.61 (dd, J = 0.5 Hz, 3.0 Hz, 1H), 3.50–3.44 (m, 1H), 1.22–1.13 ppm (m, 4H); ^{13}C NMR (100 MHz, $CDCl_3$): δ = 6.4, 27.1, 101.2, 110.5, 119.9, 121.0, 121.7, 128.2, 128.9, 137.6 ppm; IR (neat): $\tilde{\nu}$ = 3085, 3051, 3012, 1511, 1476, 1464, 1370, 1312, 1233, 1128, 1026, 764, 738, 716 cm^{-1}; MS (ES): *m/z* (%): 158 (100) $[M+H]^+$; HRMS-ES: *m/z* $[M+H]^+$ calcd for $C_{11}H_{12}N$: 158.0970, found: 158.0969.

Acknowledgements

The authors thank Professor S. P. Armes (University of Sheffield, UK) for use of the Zetasizer instrument, together with the BBSRC (grant no. BB/E014119/1) and The Home Office (contract no. 04–07–270) for their generous financial support.

Keywords: drug discovery · indoles · medicinal chemistry · prion disease · structure–activity relationships

[1] a) J. C. Watts, A. Balachandran, D. Westaway, *PLoS Pathog.* **2006**, *2*, e26 (DOI: 10.1371/journal.ppat.0020026); b) C. J. Sigurdson, M. W. Miller, *Br. Med. Bull.* **2003**, *66*, 199–212; c) S. Collins, C. A. McLean, C. L. Masters, *J. Clin. Neurosci.* **2001**, *8*, 387–397.

[2] N. J. Cobb, W. K. Surewicz, *Biochemistry* **2009**, *48*, 2574–2585.

[3] D. Vilette, *Vet. Res.* **2008**, *39*, 10 (DOI: 10.1051/vetres:2007049).

[4] a) M. C. Clarke, D. A. Haig, *Nature* **1970**, *225*, 100–101; b) D. A. Haig, M. C. Clare, *Nature* **1971**, *234*, 106–107; c) C. R. Birkett, R. M. Hennion, D. A. Bembridge, M. C. Clarke, A. Chree, M. E. Bruce, C. J. Bostock, *EMBO J.* **2001**, *20*, 3351–3358.

[5] The cell line used in this study (SMB.s15) was provided by the TSE Resource Centre at the Roslin Institute, University of Edinburgh (Edinburgh, UK); http://www.roslin.ed.ac.uk/tseresourcecentre/cell_lines.html (Last accessed: November 12, 2010).

[6] M. J. Thompson, V. Borsenberger, J. C. Louth, K. E. Judd, B. Chen, *J. Med. Chem.* **2009**, *52*, 7503–7511.

[7] G. Bonanomi, S. Braggio, A. M. Capelli, A. Checchia, R. Di Fabio, C. Marchioro, L. Tarsi, G. Tedesco, S. Terreni, A. Worby, C. Heibreder, F. Micheli, *ChemMedChem* **2010**, *5*, 705–715.

[8] clog*D* values were calculated using a freely accessible online tool; http://intro.bio.umb.edu/111-112/OLLM/111F98/newclogp.html (Last accessed: November 12, 2010).

[9] J. Bergman, J. E. Bäckvall, J. O. Lindström, *Tetrahedron* **1973**, *29*, 971–976.

[10] C. S. Rooney, W. C. Randall, K. B. Streeter, C. Ziegler, E. J. Cragoe, H. Schwam, S. R. Michelson, H. W. R. Williams, E. Eichler, D. E. Duggan, E. H. Ulm, R. M. Noll, *J. Med. Chem.* **1983**, *26*, 700–714.

[11] M. Tanaka, S. Sagawa, J. Hoshi, F. Shimoma, I. Matsuda, K. Sakoda, T. Sasase, M. Shinodo, T. Inaba, *Bioorg. Med. Chem. Lett.* **2004**, *14*, 5171–5174.

[12] a) R. M. Abdel-Motaleb, A.-M. Abdel-Salam Makhloof, H. M. Ibrahim, M. H. Elnagdi, *J. Heterocycl. Chem.* **2007**, *44*, 109–114; b) J. Slätt, I. Romero, J. Bergman, *Synthesis* **2004**, 2760–2765.

[13] F. S. Kimball, A. R. Tunoori, S. F. Victory, D. Dutta, J. M. White, R. H. Himes, G. I. Georg, *Bioorg. Med. Chem. Lett.* **2007**, *17*, 4703–4707.

[14] T. P. Karpetsky, E. H. White, *Tetrahedron* **1973**, *29*, 3761–3773.

[15] C. Sabot, K. A. Kumar, S. Meunier, C. Mioskowski, *Tetrahedron Lett.* **2007**, *48*, 3863–3866.

[16] M. J. Thompson, J. C. Louth, G. K. Greenwood, F. J. Sorrell, S. G. Knight, N. B. P. Adams, B. Chen, *ChemMedChem* **2010**, *5*, 1476–1488.

[17] a) J. H. Wynne, C. T. Lloyd, S. D. Jensen, S. Boson, W. M. Stalick, *Synthesis* **2004**, 2277–2282; b) T. Okauchi, M. Itonaga, T. Minami, T. Owa, K. Kitoh, H. Yoshino, *Org. Lett.* **2000**, *2*, 1485–1487.

[18] W. C. Guida, D. J. Mathre, *J. Org. Chem.* **1980**, *45*, 3172–3176.

[19] T. Tsuritani, N. A. Strotman, Y. Yamamoto, M. Kawasaki, N. Yasuda, T. Mase, *Org. Lett.* **2008**, *10*, 1653–1655.

[20] a) A. J. Nicoll, J. Collinge, *Infect. Disord.: Drug Targets* **2009**, *9*, 48–57; b) T. R. K. Reddy, R. Mutter, W. Heal, K. Guo, V. J. Gillet, S. Pratt, B. Chen, *J. Med. Chem.* **2006**, *49*, 607–615.

[21] F. Touil, S. Pratt, R. Mutter, B. Chen, *J. Pharm. Biomed. Anal.* **2006**, *40*, 822–832.

[22] a) K. E. D. Coan, B. K. Shoichet, *J. Am. Chem. Soc.* **2008**, *130*, 9606–9612; b) J. Seidler, S. L. McGovern, T. N. Doman, B. K. Shoichet, *J. Med. Chem.* **2003**, *46*, 4477–4486; c) S. L. McGovern, B. T. Helfand, B. Feng, B. K. Shoichet, *J. Med. Chem.* **2003**, *46*, 4265–4272; d) S. L. McGovern, B. K. Shoichet, *J. Med. Chem.* **2003**, *46*, 1478–1483; e) S. L. McGovern, E. Caselli, N. Grigorieff, B. K. Shoichet, *J. Med. Chem.* **2002**, *45*, 1712–1722.

[23] A. M. Giannetti, B. D. Koch, M. F. Browner, *J. Med. Chem.* **2008**, *51*, 574–580.

[24] A. Barret, F. Tagliavini, G. Forloni, C. Bate, M. Salmona, L. Colombo, A. De Luigi, L. Limido, S. Suardi, G. Rossi, F. Auvré, K. T. Adjou, N. Salès, A. Williams, C. Lasmézas, J. P. Deslys, *J. Virol.* **2003**, *77*, 8462–8469.

[25] a) K. Doh-ura, K. Ishikawa, I. Murakami-Kubo, K. Sasaki, S. Mohri, R. Race, T. Iwaki, *J. Virol.* **2004**, *78*, 4999–5006; b) S. J. Collins, V. Lewis, M. Brazier, A. F. Hill, A. Fletcher, C. L. Masters, *Ann. Neurol.* **2002**, *52*, 503–506.

[26] a) J. Collinge, M. Gorham, F. Hudson, A. Kennedy, G. Keogh, S. Pal, M. Rossor, P. Rudge, D. Siddique, M. Spyer, D. Thomas, S. Walker, T. Webb, S. Wroe, J. Darbyshire, *Lancet Neurol.* **2009**, *8*, 334–344; b) S. Haïk, J. P. Brandel, D. Salomon, V. Sazdovitch, N. Delasnerie-Lauprêtre, J. L. Laplanche, B. A. Faucheux, C. Soubrié, E. Boher, C. Belorgey, J. J. Hauw, A. Alpérovitch, *Neurology* **2004**, *63*, 2413–2415; c) M. Nakajima, T. Yamada, T. Kusuhara, H. Furukawa, M. Takahashi, A. Yamauchi, Y. Kataoka, *Dementia Geriatr. Cognit. Disord.* **2004**, *17*, 158–163; d) J. Benito-León, *Clin. Neuropharmacol.* **2004**, *27*, 201–203; e) H. Furukawa, T. Mitsuo, N. Masashi, Y. Tatsuo, *Nippon Rinsho* **2002**, *60*, 1649–1657.

[27] a) M. J. Waring, *Expert Opin. Drug Discovery* **2010**, *5*, 235–248; b) T. W. Johnson, K. R. Dress, M. Edwards, *Bioorg. Med. Chem. Lett.* **2009**, *19*, 5560–5564.

[28] Y. Huang, H. Okochi, B. C. H. May, G. Legname, S. B. Prusiner, L. Z. Benet, B. J. Guglielmo, E. T. Lin, *Drug Metab. Dispos.* **2006**, *34*, 1136–1144.

Received: September 9, 2010
Published online on December 8, 2010

